Journal of Asian Earth Sciences xxx (2011) xxx–xxx

Contents lists available at SciVerse ScienceDirect

Journal of Asian Earth Sciences

journal homepage: www.elsevier.com/locate/jseaes

Geomorphic Mesozoic and Cenozoic evolution in the Oka-Jombolok region (East Sayan ranges, Siberia)

M. Jolivet [a,*], S. Arzhannikov [b], A. Arzhannikova [b], A. Chauvet [c], R. Vassallo [d], R. Braucher [e]

[a] Laboratoire Géosciences Rennes, CNRS-UMR6118, Université Rennes 1, Rennes, France
[b] Institute of the Earth Crust, Irkutsk, Russia
[c] Laboratoire Géosciences Montpellier, CNRS-UMR5243, Université Montpellier II, Montpellier, France
[d] LGCA, Université de Savoie, Le Bourget du Lac, France
[e] Centre Européen de Recherche et d'Enseignement des Géosciences de l'Environnement (CEREGE), UMR-CNRS 6635, Université Paul Cézanne, Plateau de l'Arbois, 13545 Aix-en-Provence Cedex 04, France

ARTICLE INFO

Article history:
Available online xxxx

Keywords:
Paleogeomorphology
Apatite fission tracks
Cosmogenic ^{10}Be
Siberia
India–Asia collision
East Sayan ranges
Baikal Rift System

ABSTRACT

The East Sayan ranges are a key area to understand the interactions between the transpressive deformation linked to the far-field effects of the India–Asia collision and the extension linked to the opening of the Baikal Rift System. The active deformation that affects this range is very recent (around 5 Ma) but occurs in a very complex morphotectonic setting and the understanding of the Tertiary deformation relies entirely on a detailed knowledge of the pre-deformation situation. Using apatite fission track thermochronology, cosmogenic ^{10}Be and morphological study on Tertiary lava flows we demonstrate that prior to the Oligocene the morphology of the East Sayan area was characterized by a wide, constantly rejuvenated erosion surface. Apatite fission track thermal modelling indicates that this surface started to form at least in Late Jurassic–Early Cretaceous (140–120 Ma). The long-term exhumation rates (several tens of million years) derived from apatite fission track data (17.5 m/Ma) and the short-term erosion rates (over a few hundred thousand years) derived from cosmogenic ^{10}Be data (12–20 m/Ma) are coherent implying a near constant mean erosion rate since Late Jurassic. This constant, slow erosion prevented the formation of a lateritic–kaolinic weathering crust on the planation surface. By Oligocene–early Miocene times a long wavelength uplift that remains to be explained, induced incision that created shallow valleys later filled by basaltic lava flows. Finally, the present short-wavelength topography initiated during the Pliocene.

1. Introduction

West of Lake Baikal the major sinistral strike-slip Main Sayan fault reaches down to 50 km below the East Sayan ranges (San'kov et al., 2004) and separates the thick and rigid Siberian craton from the thinner, actively deforming Mongolian lithosphere (Delvaux et al., 1995, 1997; Gusev and Khain, 1996; Petit and Déverchère, 2006) (Fig. 1). The thickness of the crust vary from about 40 km north of the Main Sayan fault in the Siberian craton to about 50 km to the south in the East Sayan ranges (Polyansky, 2002). The Main Sayan fault can thus be considered as at least reaching the lithopshere. South of this fault, the Sayan ranges form an about 750 km long and 250 km wide complex that reach altitudes up to 3500 m. This elevated belt connects to the SE with the southern edge of the Baikal Rift System.

The active deformation that affects the Sayan ranges is very recent (less than 5 Ma) and results from the far field effects of the India–Asia collision to the south (Larroque et al., 2001; De Grave and Van den haute, 2002; De Grave et al., 2003; Arzhannikova et al., 2011). This transpressive deformation generates strike-slip and thrust faults within the whole Sayan ranges. However, the East Sayan ranges close to the Baikal Rift System are also locally affected by transtension leading to the formation of the Jombolok basin (Fig. 1). Arzhannikova et al. (2011) recently demonstrated that this transtensive structure results from strike-slip movements and block rotations along major E–W faults accommodating the large-scale SW–NE compressive deformation. Extension in the East Sayan ranges is thus directly linked to the far field effects of the India–Asia collision and does not result from the older still poorly understood mechanism that drove the initial opening of the Baikal Rift System (Jolivet et al., 2009).

Several studies have shown that during the Tertiary the motion along the major faults in the East Sayan ranges changed through time. For example the Tunka left-lateral normal fault (Fig. 1) that

* Corresponding author. Tel.: +33 2 23 23 67 46; fax: +33 2 23 23 67 80.
E-mail address: marc.jolivet@univ-rennes1.fr (M. Jolivet).

1367-9120/$ - see front matter © 2011 Elsevier Ltd. All rights reserved.
doi:10.1016/j.jseaes.2011.09.017

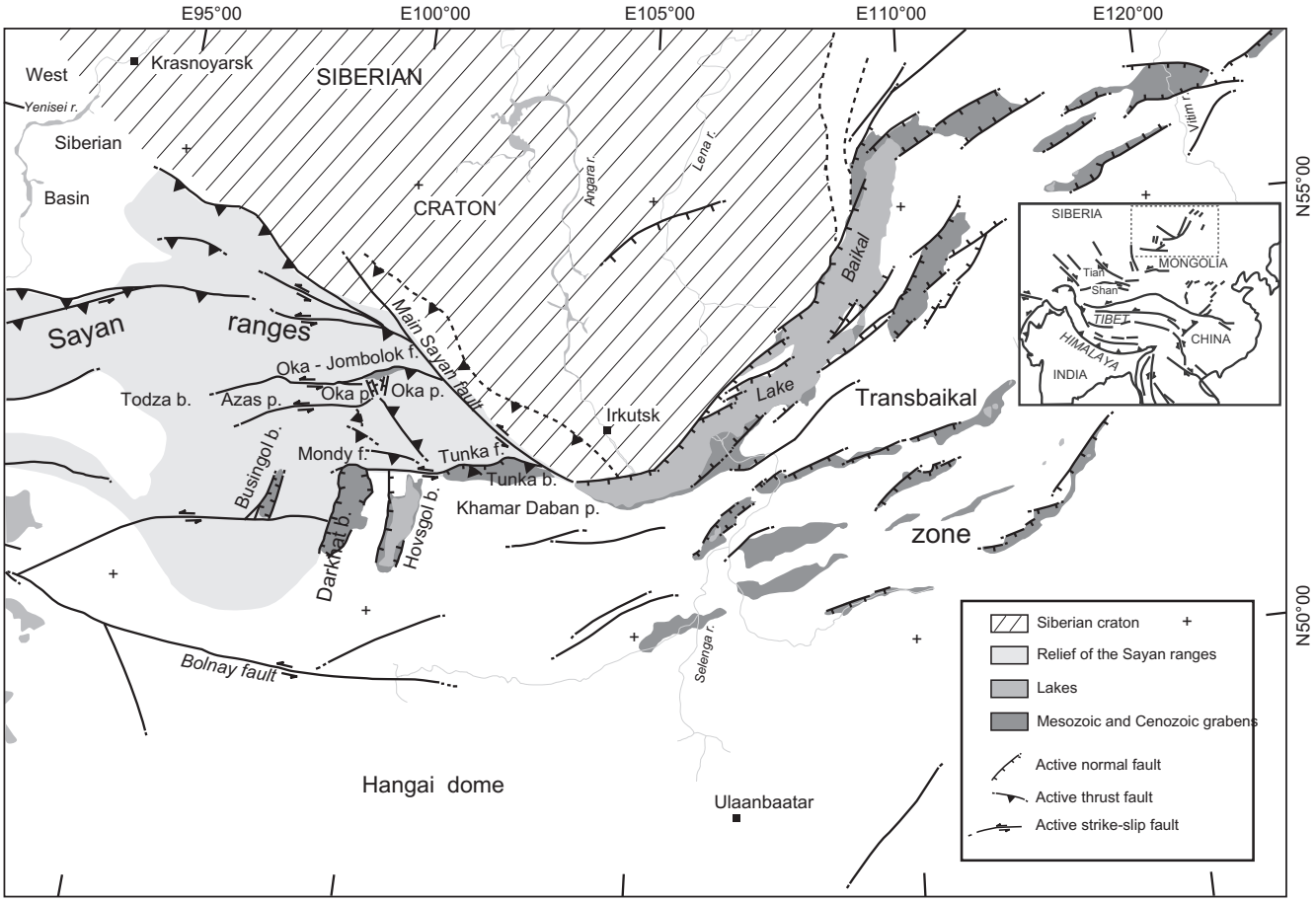

Fig. 1. General tectonic map of the Sayan and Transbaikal area. Note the contrasting tectonic regime between the transpressive Sayan region west of the southern edge of the Siberian craton and the extensive Baikal Rift System to the east. f. stands for fault; p. stands for plateau; b. stands for basin.

controls the formation of the Tunka basin shows evidence of recent (Late Pleistocene–Holocene) inversion (Larroque et al., 2001). Vertical movements along the Jombolok fault (Fig. 1) during the Late Pliocene to Pleistocene led to the growth of the Kropotkin range but since Late Quaternary, the movement becomes mainly horizontal (Arzhannikova et al., 2011).

The morphology of the East Sayan ranges is also very complex. Highly incised subranges like the Tunka or Kropotkin ranges culminating at altitudes over 3000 m coexist with large plateau-like areas such as the Oka plateau that has a mean altitude of about 2200 m (Fig. 1). The surface of those plateaus corresponds to the remnants of a large-scale pleneplanation surface apparently similar to the one developed in southern and western Mongolia during the Jurassic (Jolivet et al., 2007). However, the lateritic-kaolinic weathering crust that developed on some of these surfaces (especially to the east in the Khamar Daban area (Fig. 1)) has been dated to the late Cretaceous–Palaeogene (Mats, 1993; Kashik and Masilov, 1994; Logatchev et al., 2002) indicating that it may be younger than the Mongolian peneplanation surface.

The East Sayan ranges are a key area to understand the interactions between the transpressive deformation linked to the far-field effects of the India–Asia collision and the extension linked to the opening of the Baikal Rift System. However, due to the complex morphotectonic setting of this region the complete understanding of the Tertiary deformation in the East Sayan ranges relies entirely on a detailed knowledge of the pre-deformation situation. The purpose of this work is to establish the morphology of the Oka-Jombolok region prior to the onset of the Tertiary deformation in order to estimate which part of the present morphology may be inherited from previous deformation and uplift events and which part results from Tertiary deformation. To reach that goal we combine regional morphotectonic analysis with both thermochronological data from apatite fission tracks analysis and shorter-term denudation rates derived from cosmogenic ^{10}Be analysis (Fig. 2). While apatite fission track analysis allows calculating exhumation rates over several tens to hundreds million years (e.g. Jolivet et al., 2001, 2009, 2010; Vassallo et al., 2007a), the cosmogenic ^{10}Be analysis provides erosion rates over a period of a few hundred thousand years to about 1 Myrs (e.g. Lal, 1991; Brown et al., 1991; Siame et al., 2004; Vassallo et al., 2007b). Detailed morphological analysis of numerous lava flows present in the region coupled to the thermochronology analysis allow deciphering the Mesozoic–early Cenozoic tectonic and geomorphic evolution of this complex region of the East Sayan ranges.

2. Geological setting

2.1. Summary of the existing information on the Mesozoic to Early Cenozoic geomorphology of the East Sayan ranges

No or nearly no Jurassic sediments are exposed in the East Sayan region and all the existing paleogeographic reconstructions are based on the Jurassic deposits of both the Pre-Sayan trough on the Siberian platform and the Todza basin immediately west of the Azas volcanic region (Fig. 1). Following those reconstructions tectonic movements induced the formation of a sharp, elevated relief during the Jurassic. Erosion of that relief is represented by

Please cite this article in press as: Jolivet, M., et al. Geomorphic Mesozoic and Cenozoic evolution in the Oka-Jombolok region (East Sayan ranges, Siberia). Journal of Asian Earth Sciences (2011), doi:10.1016/j.jseaes.2011.09.017

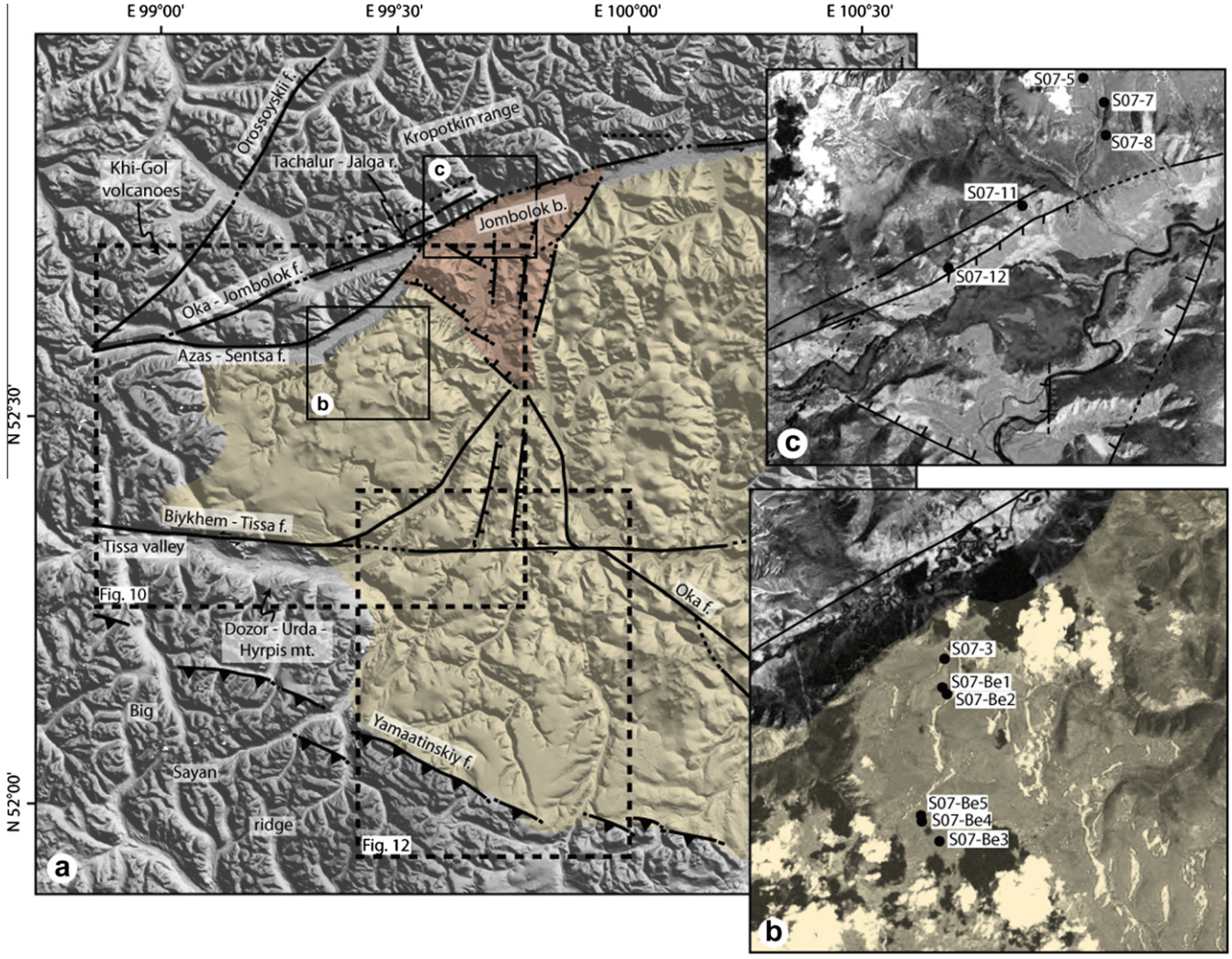

Fig. 2. General tectonic map of the Oka-Jombolok area drawn on the SRTM topographic model. The orange shaded area corresponds to the extent of the Oka plateau. The red shaded area corresponds to the Oka extension Zone (a) with position of the samples analyzed in this study for the Oka plateau (orange shaded area) (b) and the Kropotkin range (c). The plain rectangles in (a) correspond to the location of (b) and (c). The dotted rectangles correspond to Figs. 10 and 12. f. stands for fault; mt. stands for mountain; b. stands for basin. Faults are drawn from Arzhannikova et al. (2011). (For interpretation of the references to color in this figure legend, the reader is referred to the web version of this article.)

conglomerates and sandstones deposited in the Pre-Sayan trough. Some of those sediments were also deposited in intramountainous basins during Lower to Middle Jurassic and are now represented by up to 300 m thick conglomerates and coarse-grained sandtsones (Strelkov and Vdovin, 1969; Vdovin, 1976).

During Cretaceous to Eocene times a large peneplanation surface formed in the East Sayan with development of a weathering crust (Strelkov and Vdovin, 1969; Mats, 1993; Kashik and Masilov, 1994; Logatchev et al., 2002). This surface is now dismembered in several fragments such as the Oka plateau and those fragments are distributed on several altitudes, mainly 500–600 m, 800–900 m, and 1400–1600 m in the western part of the range and 1800–2200 m in the central and southern areas. This difference in altitude is potentially linked to the Cenozoic orogeny but the initial altitude of the surface (500–600 m similar to the altitude of the Siberian platform?) remains unknown.

The Cenozoic phase started during Oligocene with a general uplift of the East Sayan ranges. This uplift induced renewed erosion and the deposition of conglomerates and sandstones around the range. New valleys have been carved by erosion of the previous peneplanation surface and sediments were subsequently deposited inside those valleys (Strelkov and Vdovin, 1969; Arsentyev, 1975; Mazilov et al., 1993; Arzhannikova et al., 2011). From lower Miocene to Holocene the East Sayan range was affected by a strong magmatic activity which driving mechanism remains to be constrained (Rasskazov et al., 2000) (see Sections 2.2 and 5).

2.2. Geological setting of the Oka-Jombolok region

The Oka plateau is a 120 × 75 km large plateau area divided in two sections by the NW–SE Oka strike-slip fault (Fig. 2). To the west, the morphology of the plateau is smooth with only a few 100–300 m high hills emerging from the surface. The average altitude of this section does not exceed 2500 m. The eastern section of the plateau is higher, tilted towards the east and culminates around 2900 m. Incision of the surface is stronger than in the west with a more coherent drainage pattern. Arzhannikova et al. (2011) explained the difference in altitude by Late Pliocene thrusting along the Oka fault which uplifted the eastern section of the plateau. The lithologies exposed on the plateau are composed of Neoproterozoic and Early Paleozoic rocks (granites, gneisses and marbles) (Kuzmichev, 2004). The surface of the plateau is mostly free of sediment except for a thin (<1 m) cover of Quaternary soil and gravels.

Please cite this article in press as: Jolivet, M., et al. Geomorphic Mesozoic and Cenozoic evolution in the Oka-Jombolok region (East Sayan ranges, Siberia). Journal of Asian Earth Sciences (2011), doi:10.1016/j.jseaes.2011.09.017

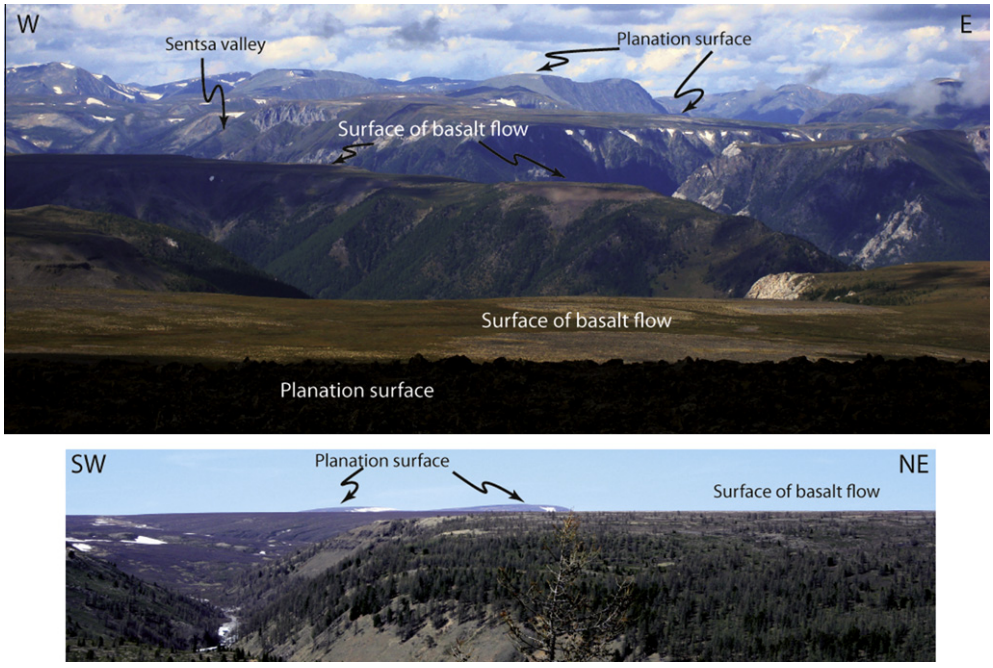

Fig. 3. Pictures of the Oka plateau. The plateau is dissected by a number of valleys (such as the Sentsa valley) and partially covered by Neogene lava flows. The planation surface is locally offset by Tertiary faults.

The top of the Oka plateau is partially covered by Neogene lava flows (Arsentyev, 1975; Kiselev et al., 1979; Rasskazov et al., 2000) (Fig. 3), some of them clearly flowing below the top of the small hills preserved on the surface. Like in the whole East-Sayan–Baikal Rift region the volcanism in the Oka–Azas region occurs in areas without visible tectonic extension. However it is clearly linked to a swarm of secondary SW–NE trending strike-slip faults (Grossvald, 1965).

Volcanism initiated in the Tunka basin during Late Cretaceous (Rassakazov, 1993) but the main episode of volcanic activity in the Oka–Azas region (as well as in the overall East Sayan–Baikal Rift region) began in the Miocene (Rasskazov et al., 2002). It occurred in several episodes (20–12 Ma, 12–7 Ma and 5.5–1.9 Ma) separated by periods of low activity (Rassakazov, 1993; Rasskazov et al., 2000; Yarmolyuk et al., 2001; Ivanov and Demonterova, 2009, 2010; Ivanov et al., 2011). Finally, Holocene lavas are also present in the Oka-Azas region (Arsentyev, 1975; Kiselev et al., 1979; Rasskazov et al., 2000; Sugorakova et al., 2003). The morphology and emplacement of these recent lava flows will be described in details below based on field observations.

Lavas are mainly subalkaline basalts, hawaiites and tholeites with some occurrences of alkaline basalts (Rassakazov, 1993; Yarmolyuk et al., 2001). Isotopic evidence as well as the petrology of the numerous lherzolite xenoliths brought to the surface by the magmas indicate that these lavas are derived from a lithospheric mantle source. The frequent periods of activity separated by periods of low activity suggest that this magmatism may correspond to a single phase of magmatism going on since 20 Ma. However the depth of the mantle-derived component as well as its percentage in the final magmas vary during time (Rasskazov et al., 2002). Ivanov and Demonterova (2010) recently demonstrated using the SiO_2 and Fe ($FeO + Fe_2O_3$) contents of the lava within the Azas region that magma generation occurred around 80 km depth (about 27 kbars). This depth increases up to about 117 km towards the north of the Baikal Rift region. These values confirm the previous value of more than 70 km for the thickness of the lithosphere (defined as the depth of the 1300 °C isotherm) under the Baikal Rift region (Ionov et al., 1995; Kiselev and Popov, 1992).

It is beyond the scope of this work to discuss the mechanism responsible for the formation of these magmas as well as their potential sources and in the following discussion we will simply use them as geomorphic markers for the evolution of the Oka-Jombolok region. However, in order to use the volcanic structures as passive markers to study the uplift history of the region, it is important to assess wether or not the magmatic activity partially controlled the tertiary uplift through underplating and isostasy. The "active rift hypothesis" proposed by a number of authors for the initiation and development of the Baikal Rift System considers that rifting is driven by mantle plume-related processes acting on the base of the lithosphere (e.g. Artemyev et al., 1978; Zorin, 1981; Logatchev and Zorin, 1987). Cunningham (2001) explained the uplift of the Hangai dome in Mongolia that started during middle Oligocene by lithospheric thinning below the Hangay craton driven by mantle flowing around an overthickenned lithospheric keel. This thinning would lead to passive asthenospheric upwarp and isostatic uplift. SKS waves analysis did not reveal the presence of such a keel (Barruol et al., 2008) but joint inversion of gravity and teleseismic data as well as geochemical analysis of the Mongolian basalts do show low velocity/density magmatic bodies below the Hangai dome (Barry et al., 2003; Tiberi et al., 2008). However, recent geophysical data do not image a wide astenospheric plume below Mongolia or the Baikal Rift System (Petit et al., 2008; Tiberi et al., 2008). Ivanov and Demonterova (2009) argue for tectonic-related uplift prior to the 17–15 Ma strong volcanic pulse in the Tuva-Mongolia region and that much of the tectonic uplift (up to 1 km) occurred after this event due to contractional tectonics between that region and the Siberian craton. In the Bokson river area south of the Big Sayan ridge, two episodes of uplift occurred before the onset of the Miocene (20 Ma) and before the Pliocene (5 Ma) volcanic events (Ivanov and Demonterova, 2009). A period of regional uplift preceding a strong volcanic activity could well be related to the isostatic compensation effects of underplated magmas at the base of the crust. However, as noted by Ivanov and Demonterova (2009) most of the uplift in the Tuva-Mongolia region occurred after the Miocene volcanic event which is not consistent with the fact that surface eruption would decrease the

Please cite this article in press as: Jolivet, M., et al. Geomorphic Mesozoic and Cenozoic evolution in the Oka-Jombolok region (East Sayan ranges, Siberia). Journal of Asian Earth Sciences (2011), doi:10.1016/j.jseaes.2011.09.017

amount of underplated magma and thus induce a negative isostatic effect. They showed that volcanism in the Mongolia – Baikal region occurred at different times during the Tertiary in relation with tectonic movements between small-scale lithospheric blocks. Magma underplating generating isostatic uplift would thus have to be correlated with local scale deformation and not with a passive, large scale melting process occurring in the lithospheric mantle. We cannot exclude the fact that isostatically driven uplift may be responsible for some part of the uplift of the Azas–Oka-Jombolok region but the short wavelength topography we are mostly interested in appears clearly driven by tectonic forces. Keeping this in mind we will consider the volcanic structures of the Oka-Jombolok region as passive topographic markers.

To the north, the Oka-Jombolok fault separates the Oka plateau from the 3000 m high Kropotkin range (Fig. 2). The eastern termination of the fault connects with the Main Sayan fault. The kinematic of the Oka-Jombolok fault is very complex and variable through time (e.g. Grossvald, 1965; Chipizubov and Serebrennikov, 1990; Parfeevets and Sankov, 2006). Arzhannikova et al. (2011) recently proposed that the fault was mainly transpressive with only minor horizontal displacement through Late Pliocene–Pleistocene, leading to the topographic growth of the Kropotkin range. By Late Quaternary, the kinematics of the Oka-Jombolok fault changed to nearly pure sinistral strike-slip. This strike-slip faulting, associated to rotation of some small, rigid blocks induced the formation of local extension zones such as the Jombolok basin (or Oka Extension Zone) (Fig. 2).

The Jombolok basin and valley are filled by several stacked lava flows (Fig. 4). These lavas originated some 75 km to the west in the upper Khi-Gol and Jombolok valleys along the SW–NE trending Orossoyskiy fault (Fig. 2) (Arsentyev, 1975; Kiselev et al., 1979; Rasskazov et al., 2000; Ivanov et al., 2011). The lava flow issued from several eruption centers spread along the Khi-Gol and Jombolok valleys, probably related to the extensive Azas lava plateau situated to the west of the Oka plateau (Rasskazov et al., 2000). Our own field investigation as well as previous studies by Sugorakova et al. (2003) and Ivanov et al. (2011) revealed that magmatism occurred in several episodes producing four lava flows. Fig. 4 shows a series of small-scale secondary flows occurring on the main lava body. The latest activity in the Khi-Gol volcanic center, that produced the major Jombolok lava flow has been dated at 7130 ± 140 cal ^{14}C years BP (Ivanov et al., 2011). Within the Jombolok basin, trees and grass have already colonized the main volcanic body called hereafter the «old» flows while the secondary flows (or «young» flows) do not host any vegetation. This indicates that the young flows are indeed much younger than the old flows and are probably less than a few hundreds of years old (Fig. 4). The apexes of all the young flows are systematically aligned parallel to the Oka-Jombolok fault. The old and young lavas are flowing towards the SE following the actual slope of the basin and no change in that slope can be evidenced between the two generations of lavas. While it appears easy to understand the shape of the old flows, it is more difficult to explain the geometry of the young flows. The spreading centers of the young flows are not obvious in the field and two hypotheses are suggested:

– Most young flows are filling depressions inside the old flows (some of them even forming temporary lakes) and their edges are formed by local topographic ridges that may be interpreted as lava tubes inside the large old flow. These tubes would have allowed the lava to be transported from further up in the Jombolok valley towards the Jombolok basin where they would have finally ruptured spreading the young lava flows. Given the orientation of the apexes of the flows breaking of the lava tubes may have been induced by a fault inside the Jombolok basin, parallel to the main Oka-Jombolok fault.

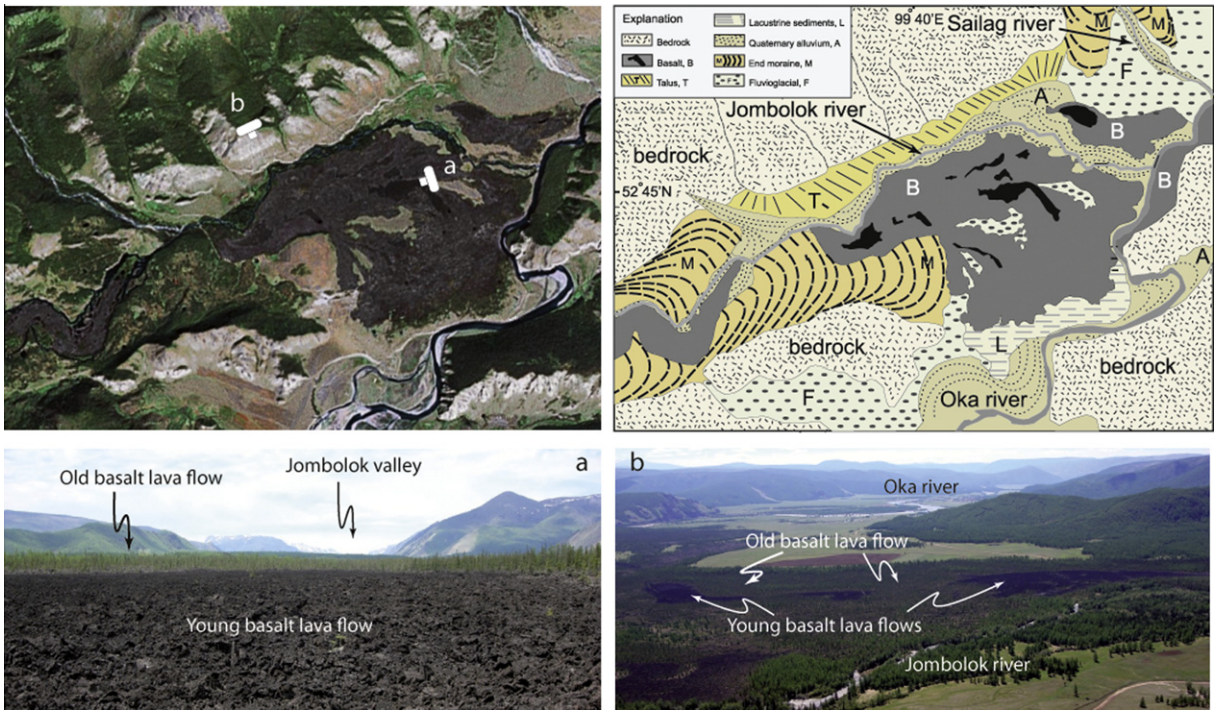

Fig. 4. Neogene and Quaternary lava flows in the Jombolok basin. Top left: Google Earth® picture of the basin showing the basalt flows in dark. (a) and (b) refer to the pictures below. Top right: geomorphic interpretation of the aerial picture showing the chronology between the various lava flows and the emplacement of the glacial moraines and river sediments. The youngest basalt flows are indicated in black on top of the oldest ones. Pictures (a) and (b): close and large view of the two sets of lava flows in the Jombolok basin. While the oldest ones are covered by saplings, the youngest ones are free of vegetation, soil or any sort of sediments implying that they are probably only a maximum of a few hundred years old.

Please cite this article in press as: Jolivet, M., et al. Geomorphic Mesozoic and Cenozoic evolution in the Oka-Jombolok region (East Sayan ranges, Siberia). Journal of Asian Earth Sciences (2011), doi:10.1016/j.jseaes.2011.09.017

– The second hypothesis considers that the magmas from the young flows did not originated from a spreading center further up in the valley (Rasskazov et al., 2000) but was brought to the surface along fractures parallel to the Oka-Jombolok fault. The various lavas that originated from the Azas plateau are linked to a swarm of secondary SW–NE trending strike-slip faults (Grossvald, 1965) (see below), a direction consistent with the direction of alignment of all the apexes of the young flows in the Jombolok basin.

We do not have enough information to clearly choose between those two hypotheses and further work will be necessary especially on characterizing the spreading centers of the young flows.

3. Fission track thermochronology

3.1. Methodology

The apatite samples were mounted on glass slides using epoxy glue and polished. Samples were etched in 6.5% HNO_3 (1.6 M) for 45 s at 20 °C to reveal the spontaneous fission tracks (Seward et al., 2000), before being irradiated with a neutron fluence rate of 1.0×10^{16} neutrons/cm^2 (Oregon State University, Oregon, USA). The micas used as external detector were etched in 40% HF for 40 min at 20 °C in order to reveal the induced fission tracks. The ages were calculated following the method recommended by the Fission Track Working Group of the IUGS Subcommission on Geochronology (Hurford, 1990) using the zeta calibration method (Hurford and Green, 1983). CN5 glass was used as dosimeter. Ages were calculated using an overall weighted mean zeta value of 351 ± 20 a cm^2 (MJ), obtained on both Durango (McDowell et al., 2005) and Mount Dromedary apatite standards (Green, 1985; Tagami, 1987). Fission tracks were counted using the Autoscan© software (on manual mode) on a Zeiss M1 microscope, with a magnification of 1250 under dry objectives. All ages are central ages and errors are quoted at 2σ (e.g. Galbraith and Laslett, 1993; Galbraith, 2005). Data are reported in Table 1.

Thermal history modelling was done using the QTQt software (Gallagher et al., 2009) with the Ketcham et al. (2007) multikinetic annealing model that takes into account the D_{par} parameter (see below). Variation in fission track annealing (and thus in apparent fission track age and mean track lengths) is correlated with the apatite cell parameters and is thus linked to crystallographic structure (e.g. Green and Durrani, 1978; Green, 1981; Donelick, 1991). For that reason, as a general standard only crystal sections that are parallel to the ⟨c⟩ crystallographic axis have been analyzed (for age determination and for track length measurements). Fission tracks are distributed in all directions within the apatite crystals but to provide an accurate length measurement only horizontal tracks parallel to the sample's surface and confined into the crystal (i.e. that do not cross the surface and are thus not partially cut) were measured (track length measurements are c-axis projected values). Measurements were performed under reflected light at 1250× magnification (dry) and using the Autoscan© system (on manual mode). The track lengths distribution histograms are presented in Fig. 5. The apatite chemical composition, and especially the Cl and F content also controls the annealing properties of the fission tracks (Donelick, 1993; Burtner et al., 1994; Barbarand et al., 2003). For example an increase in Cl content will slow down the annealing process and increase the apparent fission track age, the mean track length and the track diameter relatively to a more F-rich apatite. Variations in the fission tracks sensitivity to annealing can thus be deduced from variations of the fission track diameter. The D_{par} used as an input parameter in the QTQt model corresponds to the diameter (measured on sections parallel to the c-axis) of the etched trace of the intersection of a fission track with the surface of the analyzed apatite crystal measured parallel to the c-axis. Measurements were performed using a magnification of 2000×. Each D_{par} value reported in Table 1 represents the mean value of 50–100 measurements.

The Ketcham et al. (2007) annealing model relies on track lengths and D_{par} measured after etching by a 5.5 M HNO_3 acid during 20 s (Donelick et al., 1999) whereas we used the 1.6 M HNO_3 acid/45 s etching protocol. While the etching parameters can be controlled well enough to have only a negligible effect on the measured mean fission track length, it does have a strong effect on the D_{par} value (Sobel and Seward, 2010). For that reason we corrected the measured D_{par} values following the method of Sobel and Seward (2010) to fit with the Ketcham et al. (2007) annealing model. The correction factor is 0.825 and corrected D_{par} values are reported in Table 1.

The annealing models and thus the thermal histories are only valid within the apatite partial annealing zone (PAZ) temperature range and the portion of the cooling curve obtained outside the PAZ should not be interpreted. The PAZ can be defined as the temperature interval within which the fission tracks anneal at a rate compatible with the geological time scale. It is generally comprised between 110 ± 10 °C and 60 °C (e.g. Green et al., 1989; Corrigan, 1991) but these values can slightly change due to the above-mentioned variations in the apatite chemical composition. For temperatures higher than about 110 °C, fission tracks will anneal nearly instantaneously compared to the geological time scale wile for temperatures below about 60 °C the annealing rate will be extremely low.

Table 1
Apatite fission track results. Lat./Long. are the latitude and longitude of each sample. Altitude is the sampling altitude in meters. Nb is the number of crystals analyzed. ρ_d is the density of induced fission track density (per cm^2) that would be obtained in each individual sample if its U concentration was equal to the U concentration of the CN5 glass dosimeter. Number in brackets is the total number of tracks counted. ρ_s and ρ_i represent sample spontaneous and induced track densities per cm^2. Number in brackets is the total number of tracks counted. [U] is the calculated uranium density (in ppm). $P(\chi^2)$ is the probability in % of χ^2 for ν degrees of freedom (where ν = number of crystals − 1). D_{par} is the mean fission-track pit diameter in μm corrected following Sobel and Seward (2010) using a correction factor of 0.825. MTL is the measured mean fission-track length in μm. Track lengths measurements were performed on horizontal confined fission tracks in crystal sections parallel to the c-crystallographic axis. Length values are c-axis projected values. Error is ±1σ. Number in brackets is the total number of tracks measured. Std. is the standard deviation for the track lengths measurements. FT age is the apatite fission-track age in Ma. Ages have been calculated using the Trackkey software (Dunkl, 2002). Error is ±2σ.

Sample	Rock type	Lat./Long.	Altitude	Nb	$\rho_d \times 10^4$ cm^{-2}	$\rho_s \times 10^4$ cm^{-2}	$\rho_i \times 10^4$ cm^{-2}	[U]	$P(\chi^2)$ (%)	D_{par} (μm)	MTL (μm)(±1σ)	Std. (μm)	FT age (Ma) (±2σ)
S07-3	Granite	N52°35′14.7″/E099°25′29.3″	2009	25	142.6 (10,533)	41.39 (601)	83.2 (1208)	7	71	1.0	13.1 ± 0.1	1.71	123.5 ± 9.6
S07-5	Granite	N52°49′52.0″/E099°43′42.3″	2348	14	139.7 (10,533)	42.74 (106)	121.77 (302)	12	75	2.8	12.8 ± 0.1	2.00	85.6 ± 10.9
S07-7	Granite	N52°48′51.3″/E099°44′34.6″	2113	28	130.9 (10,533)	31.43 (182)	83.59 (484)	8	83	1.7	13.3 ± 0.1	1.93	85.9 ± 9.0
S07-8	Granite	N52°48′45.2″/E099°44′47.1″	2034	25	129.5 (10,533)	54.82 (358)	145.48 (950)	14	48	1.2	12.7 ± 0.1	2.10	85.2 ± 7.4
S07-11	Paragneiss	N52°46′50.0″/E099°41′11.3″	1735	12	138.2 (10,533)	242.53 (747)	505.52 (1557)	44	5	1.0	12.5 ± 0.1	1.83	114.6 ± 9.5
S07-12	Granite	N52°45′29.1″/E099°39′10.7″	1464	20	135.3 (10,533)	87.64 (546)	260.03 (1620)	23	55	1.0	12.9 ± 0.1	1.72	79.6 ± 6.2

Please cite this article in press as: Jolivet, M., et al. Geomorphic Mesozoic and Cenozoic evolution in the Oka-Jombolok region (East Sayan ranges, Siberia). Journal of Asian Earth Sciences (2011), doi:10.1016/j.jseaes.2011.09.017

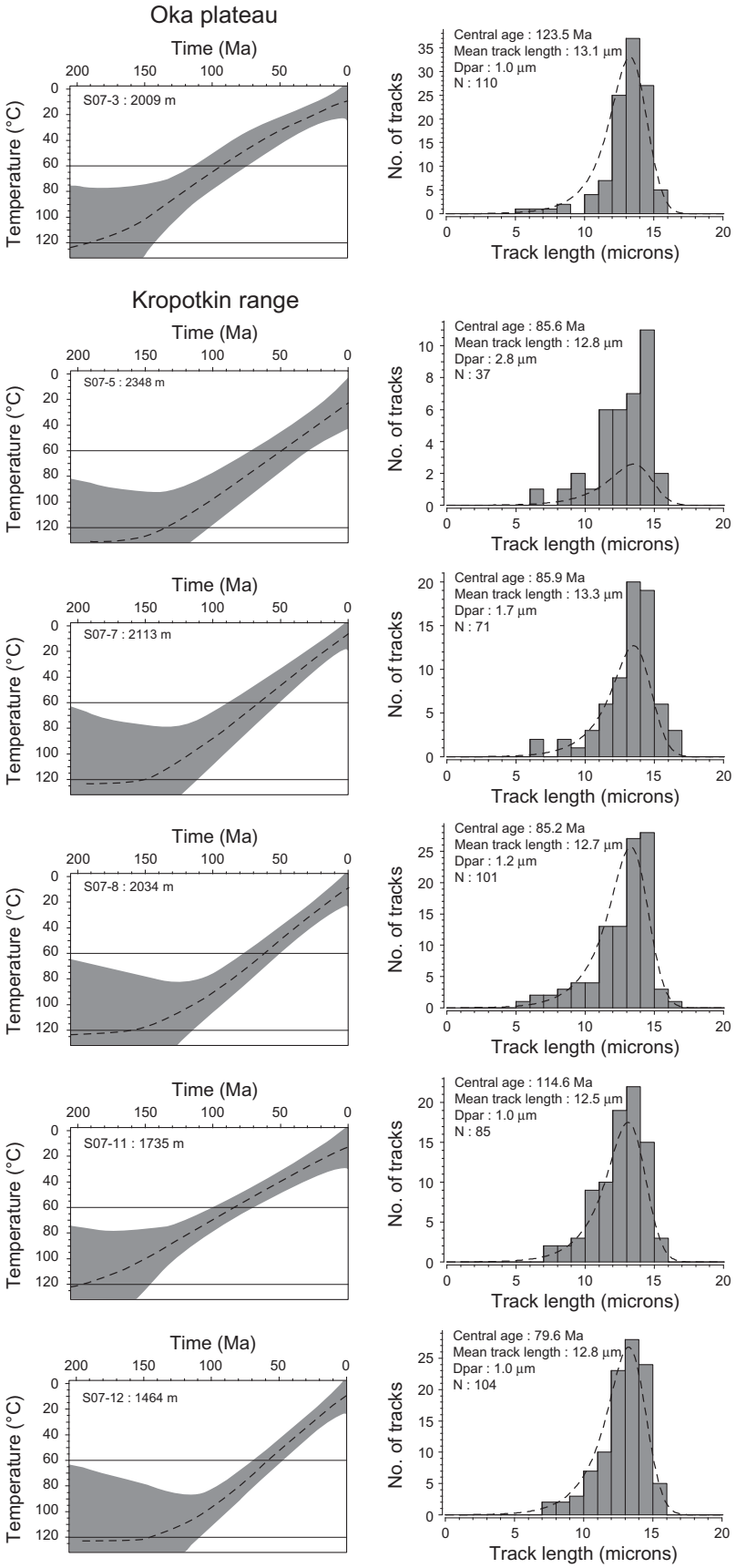

Fig. 5. Apatite fission track thermal modelling results of individual samples from the Oka plateau and the Kropotkin range. *N*, number of track lengths measured. The histograms correspond to the measured data while the dashed line corresponds to the calculated data. The gray envelope on the thermal models corresponds to the 95% credible expected thermal histories (Gallagher et al., 2009). The dashed line on the models corresponds to the average of all the models sampled. The horizontal lines indicate the limits of the apatite partial annealing zone. Models are only valid within this temperature range. See text for complete discussion of the results.

Please cite this article in press as: Jolivet, M., et al. Geomorphic Mesozoic and Cenozoic evolution in the Oka-Jombolok region (East Sayan ranges, Siberia). Journal of Asian Earth Sciences (2011), doi:10.1016/j.jseaes.2011.09.017

3.2. Results

The fission track samples were collected both on the Oka plateau and on the southern edge of the Kropotkin range along the scarp of the Jombolok fault. To prevent any thermal effect on the fission track system, all samples were collected away from the numerous lava flows that occur in the region. Sample locations are indicated in Fig. 2 and in Table 1.

Sample S07-3 is a granite collected on the surface of the Oka plateau (Fig. 2). It shows a central age of 123.5 ± 9.6 Ma and a mean track length of 13.1 ± 0.1 μm with a standard deviation of 1.71 μm and a D_{par} of 1.0 μm (Table 1). The track length distribution is unimodal (Fig. 5) which, associated to the relatively high mean track-length is typical of a simple one-phase exhumation history (e.g. Galbraith and Laslett, 1993). However a number of short track lengths (shorter than 10 μm) indicate a long period of residence within the PAZ.

Samples S07-5, S07-7, and S07-8 are all granites collected along a 350 m high subvertical profile on the southern edge of the Kropotkin range (Fig. 2). Central ages are similar from 85.9 ± 9 Ma to 85.2 ± 7.4 Ma with mean track lengths ranging from 13.3 ± 0.1 to 12.7 ± 0.1 μm, a standard deviation ranging from 2 × 10 to 1.93 μm and a D_{par} ranging from 2.8 to 1.2 μm (Table 1). Like for sample S07-3 the track lengths distribution is unimodal (Fig. 5) but, except for sample S07-7 shows a higher number of medium to short tracks. This is consistent with the slightly higher standard deviations. All together those parameters are indicative of a simple exhumation history marked by a long stage in the PAZ.

Sample S07-11 is a two micas paragenesis collected further down and west from the previous profile, close to the Jombolok fault into a block separated from the main Kropotkin range by a secondary fault parallel to the Jombolok fault (Fig. 2). Sample S07-11 which has a low D_{par} of 1.0 μm shows a central age of 114.6 ± 9.5 μm (Table 1) older than the ages obtained on the subvertical profile but younger than the age of sample S07-3 from the Oka plateau. The mean track length is 12.5 ± 0.1 μm with a standard deviation of 1.83 μm (Table 1).

Sample S07-12 is a granite collected immediately near the Jombolok fault at the bottom of the scarp formed by the Jombolok fault but still in the Kropotkin range. It shows a central age of 79.6 ± 6.2 Ma slightly younger than the age of the samples from the subvertical profile but still within the error margin. The mean track lengths value is 12.9 ± 0.1 μm with a standard deviation of 1.72 μm and again a low D_{par} of 1.0 μm (Table 1). The track lengths distribution is again unimodal.

Thermal modelling of the fission track data provides a statistical but more complete temperature-time history of the Oka plateau and the southern Kropotkin range (Fig. 5). As already suggested by the age and track lengths data, all the samples display a monotonous slow cooling through the PAZ. To prevent any enforcement of the model a single, wide temperature-time constraint (a temperature–time «box» in which the model as to pass through) was used in the model ranging from 250 to 150 Ma and 180 to 60 °C.

Sample S07-3 from the Oka plateau entered the PAZ during Early Jurassic and crossed the 60 °C isotherm during Late Cretaceous.

Samples from the Kropotkin range have a similar thermal history. They entered the PAZ during Late Jurassic (around 160–140 Ma) and slowly cooled down until they left the PAZ in Late Cretaceous (between 70 and 60 Ma). This is consistent with a homogeneous exhumation of the Kropotkin range, samples S07-5, S07-7, S07-8 and S07-12 belonging to a single block. Sample S07-5 at the top of the profile seems to have a slightly younger history. However, due to the very bad quality of the apatite crystals in that samples (occurrence of numerous inclusions and very small size of the crystals) only 14 individual ages and 37 track lengths were obtained. This could account for small variations and inconsistences in the modelled thermal history.

Sample S07-11 has a thermal history nearly identical to the history of sample S07-3 confirming that the isolated block along the southern edge of the Kropotkin does not follow the same exhumation pattern as the range itself (illustrated by the exhumation of samples S07-5, S07-7, S07-8 and S07-12).

The QTQt software allows to model together all the samples from a vertical profile. Each individual sample is considered as part of a homogeneous section of crust submitted to a unique thermal history. The software considers the vertical distance between the samples as constant through time and uses all the available age, track lengths and D_{par} data to constrain the thermal history of the block. Fig. 6a shows an integrated cooling history for samples S07-5, S07-7, S07-8 and S07-12 that we considered as part of the same block. Because of its obviously different exhumation history sample S07-11 was not considered in that model.

As expected the resulting model clearly shows a slow exhumation pattern during the Mesozoic and early Cenozoic. The integration of all the samples into a single data pool allows to better constraint the high-temperature part of the cooling history and the entry into the PAZ seems to occur around 130–120 Ma thus later than previously estimated from the individual samples (Fig. 5). This age remains similar (140–125 Ma) when sample S07-5 which is less constrained than the other ones (14 grains counted and only 37 tracks lengths measured) is excluded from the model (Fig. 6b).

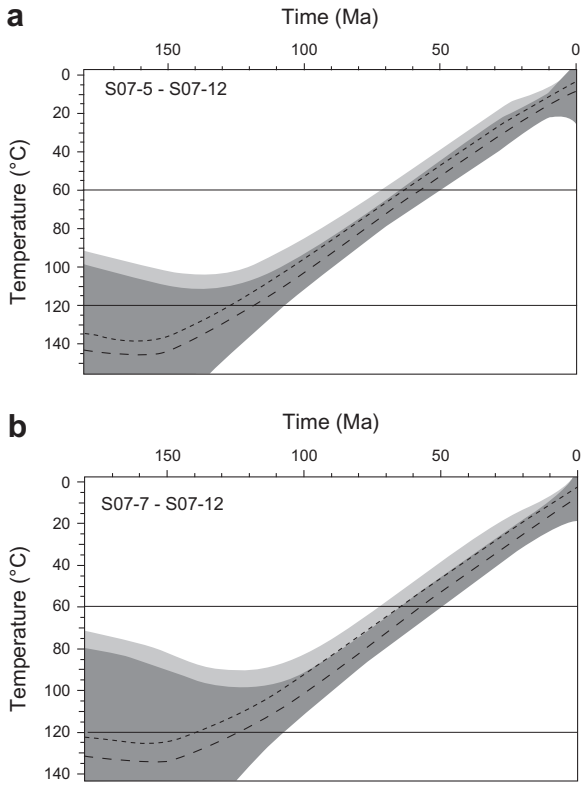

Fig. 6. Integrated thermal model for the Kropotkin profile. (a) Model including samples S07-5, S07-7, S07-8 and S07-12. The light-gray envelope corresponds to the 95% credible expected thermal histories for the upper sample (S07-5) and the dark-gray envelope to the 95% credible thermal histories for the lower sample (S07-12). The upper dashed line corresponds to the average of all the models sampled for the upper sample. The lower dashed line corresponds to the average of all the models sampled for the lower sample. (b) Similar model but excluding sample S07-5. See text for a complete discussion.

Please cite this article in press as: Jolivet, M., et al. Geomorphic Mesozoic and Cenozoic evolution in the Oka-Jombolok region (East Sayan ranges, Siberia). Journal of Asian Earth Sciences (2011), doi:10.1016/j.jseaes.2011.09.017

Table 2
Cosmogenic ^{10}Be results.

Sample[a]	Type of sample	Altitude (m)	Latitude/longitude	Stone scaling	^{10}Be[b] (at/g)	Uncertainty (at/g)	Denudation rate (m/Myrs)	Denudation uncertainty (m/Myrs)
S07-Be1	Quartz pebble	2308	N52°33′51.4″/E099°26′41.5″	6.75	4.796E+06	0.758E+05	3.88	0.06
S07-Be2	Quartz pebble	2340	N52°33′43.1″/E099°26′55.3″	6.90	1.237E+06	0.321E+05	16.95	0.44
S07-Be3	Granite	2481	N52°31′15.3″/E099°25′48.5″	7.59	1.748E+06	1.585E+05	13.01	1.18
S07-Be4	Granite	2279	N52°31′35.6″/E099°24′59.8″	6.62	6.175E+06	43.666E+05	2.85	0.18
S07-Be5	Granite	2275	N52°31′42.1″/E099°24′53.6″	6.60	1.062E+06	0.303E+05	19.00	0.54

[a] Rock density of 2.5 g/cm^3. Average thickness: 3 cm. Topographic shielding factor = 1.
[b] AMS measurements were performed at the French AMS National Facility, ASTER, located at the CEREGE in Aix-en-Provence. Beryllium data were calibrated directly against the National Institute of Standards and Technology (NIST) beryllium standard reference material 4325 by using an assigned value of $(2.79 \pm 0.03) \times 10^{-11}$; associated blank ratio is 3.15×10^{-15}.

4. ^{10}Be analysis

The half-life of in situ produced cosmogenic ^{10}Be nuclide (1.387 Ma (Chmeleff et al., 2010; Korschinek et al., 2010)) allows dating surficial rocks over a few hundreds of thousand years. In surficial rocks the cosmogenic isotope concentration increases with time until the loss in atoms due to radioactive decay and erosion compensates the formation of new atoms within the rock. When this steady state equilibrium is reached a mean erosion rate (which is inversely proportional to the isotope concentration) can be derived (Brown et al., 1995). In order to constrain the Late Quaternary (Late Pleistocene–Holocene) erosion rates on the Oka plateau we measured the in situ produced cosmogenic ^{10}Be concentrations within quartz from granite boulders (samples S07-Be3, S07-Be4 and S07-Be5) or quartz cobbles (samples S07-Be1 and S07-Be2) exposed on the Oka plateau (e.g. Lal, 1991; Ritz et al., 2006; Vassallo et al., 2007a). Boulders were selected as large as possible and encased in the matrix with only the top part standing out of the ground surface. As the samples were collected on a flat topography in the most elevated regions of the mountain range, topographic shielding is neglected here (Dunne et al., 1999).

The chemical treatment of the samples and the AMS measurements were carried out at the CEREGE laboratory in Aix-en-Provence. Samples were prepared for cosmogenic nuclide concentration measurements following chemical procedures adapted from Brown et al. (1991) and Merchel and Herpers (1999). All the data reported in this study (Table 2) have been measured at ASTER (CEREGE, Aix-en-Provence). After addition in each sample of ~100 µl of an in-house 3×10^{-3} g/g ^{9}Be carrier solution prepared from deep-mined phenakite (Merchel et al., 2008), all ^{10}Be concentrations were normalized to ^{10}Be/^{9}Be SRM 4325 NIST standard with an assigned value of $(2.79 \pm 0.03) \times 10^{-11}$ (Nishiizumi et al., 2007). This standardization is equivalent to 07KNSTD within rounding error.

Cosmocalc add-in for Excel (Vermeesch, 2007) has been used to calculate sample thickness scaling (with an attenuation coefficient of 160 g cm^{-2}) and atmospheric pressures. Ston, 2000 polynomial law has been used to determine surficial production rate assuming a SLHL production rate of 4.49 at/g/yr for ^{10}Be ($T1/2 = 1.387$ Ma).

Denudation rates (spanning a time range of several hundred thousand years) derived from ^{10}Be analyses vary from 2.85 ± 0.18 m/Myrs to 19.00 ± 0.54 m/Myrs with no observable difference between the quartz samples and the granite samples. Samples S07-Be1, S07-Be2 and S07-Be3 were collected from the top of small, about 200 m high hills occurring on the generally flat plateau surface while samples S07-Be4 and S07-Be5 were sampled on the main plateau surface. Once more there is no apparent correlation in calculated erosion rates and the position of the samples.

Overall the calculated erosion rates are very low with a mean value of about 12 m/Myrs and a maximum value of about 20 m/Myrs similar to the 23.6 ± 3 m/Myrs value calculated for the 4000 m high Ih Bogd plateau in the Gobi Altay (Jolivet et al., 2007; Vassallo et al., in press). Considering the mean cooling curve obtained from fission track modelling of sample S07-3 from the Oka plateau and a mean geothermal gradient of 30 °C km^{-1}, the mean exhumation rate between 190 Ma and 0 Ma would be of 17.5 m/Myrs, thus very similar to the much shorter term erosion rate calculated from ^{10}Be data. The interesting result is that even if the instantaneous erosion rate probably varied during this huge time interval as a consequence of the climatic oscillations, longer term (fission tracks data describe the exhumation rates from Cretaceous to Present) and shorter term (cosmogenic ^{10}Be data describe erosion rates from Late Pleistocene to Holocene) data are consistent with a slow erosion in the Oka region. This major result seems to contradict the observed rejuvenation of the relief during the Cenozoic. However, the cosmogenic ^{10}Be data have been obtained on the undeformed Oka plateau and not from the actively uplifted ranges surrounding it where Pleistocene to Holocene erosion rates are certainly much higher. Ivanov and Demonterova (2009) calculated incision rates (over the last 5 Ma) of 30 m/Myrs in the Oka river and 70 m/Myrs for the Belaya river connected with the Siberian platform further to the NE. They also calculated a Miocene (16–13 Ma) uplift rate of 40 m/Myrs in the Hovsgol area. All those values are 3–4 times higher than the erosion rate calculated for the Oka plateau but this is consistent with both the incision of the valleys within the initial surface of the plateau and the progressive uplift of the remnants of that surface.

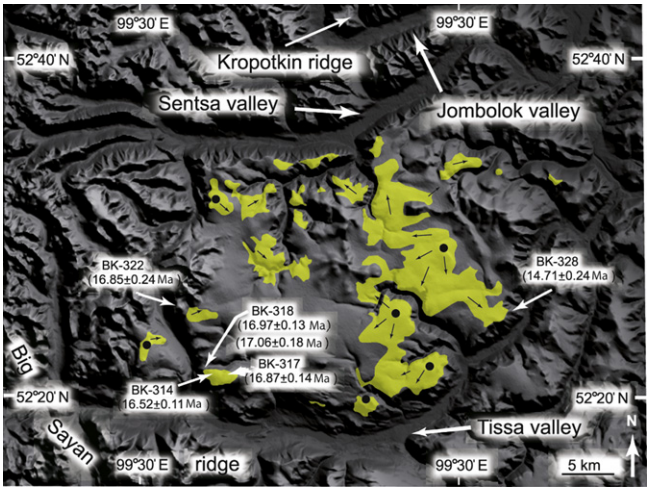

Fig. 7. SRTM® topographic map of the Neogene lavas (in yellow) on top of the Oka plateau between the Sentsa-Jombolok valley and the Tissa valley (SJT plateau area). Ages are from Rasskazov et al. (2000) and from Ivanov and Demonterova (2009). See Fig. 2 for location. (For interpretation of the references to color in this figure legend, the reader is referred to the web version of this article.)

Please cite this article in press as: Jolivet, M., et al. Geomorphic Mesozoic and Cenozoic evolution in the Oka-Jombolok region (East Sayan ranges, Siberia). Journal of Asian Earth Sciences (2011), doi:10.1016/j.jseaes.2011.09.017

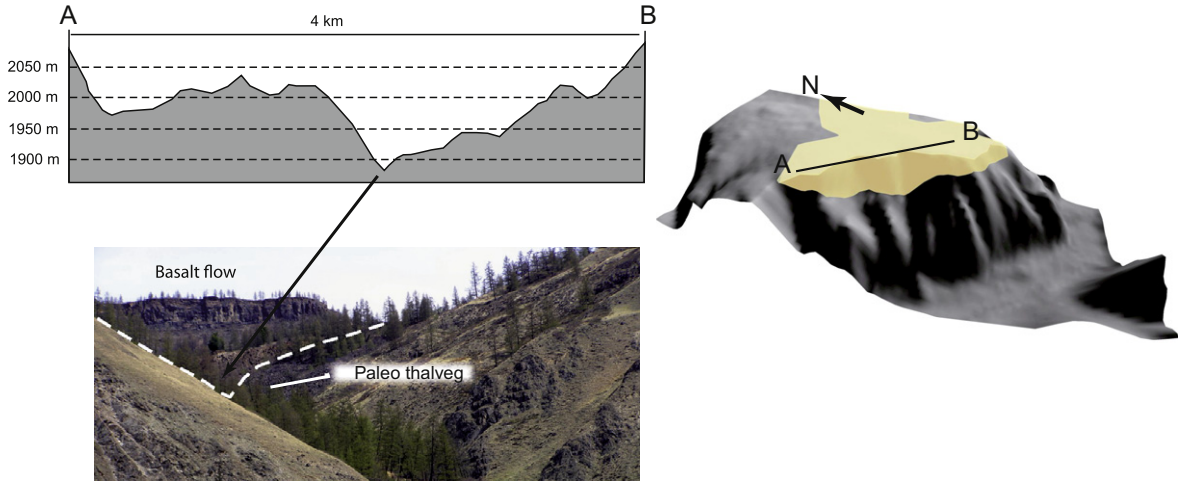

Fig. 8. Example of a natural section across a basalt lava flow (in yellow on the SRTM® topographic model) filling a paleovalley on top of the Oka plateau. The topographic profile has been drawn in an area where the lava flow has been eroded away and closely corresponds to the pre-lava profile of the valley. (For interpretation of the references to color in this figure legend, the reader is referred to the web version of this article.)

5. Volcanism and Tertiary paleotopography

Deep post middle Miocene (post 10 Ma) incisions inside and around the Oka plateau provide opportunities to reconstruct the topography of the surface below the Miocene lava flows that cover the plateau. Direct field observations have been completed by SRTM data, geological maps informations (VSEGEI, 1975) and Landsat™ images.

The first basaltic flows, erupted between 20 and 12 Ma are situated in the west, north and east of the Oka plateau (Fig. 7) and are the topographically highest flows (Rasskazov et al., 2000; Ivanov and Demonterova, 2010). Those hundreds of meters thick flows capped and preserved from erosion large surfaces of the pre-existing topography which allows us to reconstruct relatively accurately the general early Miocene relief (Fig. 8). Within this first group we especially concentrated on the basalt plateaus situated between the Sentsa-Jombolok and Tissa valleys (SJT plateau) (Fig. 7) and between the Dibi and Tissa valleys (DT plateau) (Fig. 9), dated between 17 and 14 Ma using K–Ar and ^{40}Ar–^{39}Ar (Rasskazov et al., 2000; Ivanov and Demonterova, 2010).

The SJT plateau is limited to the north by the Kropotkin range and to the south and west by the Big Sayan Ridge. The mean elevation of the plateau is 2250 m with several isolated summits reaching 2500 m. The basaltic flows are separated by a series of low-relief NW–SE trending ridges. Using the surface topography of the flows we determined five eruption centers as well as the flowing direction of the associated lavas (Fig. 7). These lavas are implaced inside 150–200 m paleovalleys (Fig. 8) previously incised into the generally flat surface of the plateau. This observation is consistent with the results of Ivanov and Demonterova (2010) which report the emplacement of 17–15 Ma old flows within 100 m deep valleys east of the Oka plateau, close to the Main Sayan fault. These lavas were flowing towards the NE indicating that the general slope in that region was towards the Siberian platform (Vdovin, 1976).

Further south the DT plateau is separated in two parts by the Balahta valley (Fig. 9). The 600–700 m deep incision of the Tissa and Balahta valleys provide good sections of the pre-volcanic topography. On the SE side of the Tissa valley, a 100–200 m deep paleovalley is filled by a lava flow (Fig. 10). The same paleovalley is also visible on both sides of the Balahta valley revealing that incision increases from NW to SE potentially indicating that the paleoriver was flowing in that direction (Fig. 11). In the Balahta valley the paleoincision is 4–5 km large and 300–400 m deep.

Numerous 10–11 Ma flows are exposed on the eastern part of the DT plateau (Rasskazov et al., 2000). The eruption center is the Shirokaya volcanoe (Fig. 9) and the lavas generally flowed towards the SE. However, some of the flows were directed towards the north, following a paleovalley corresponding more or less to

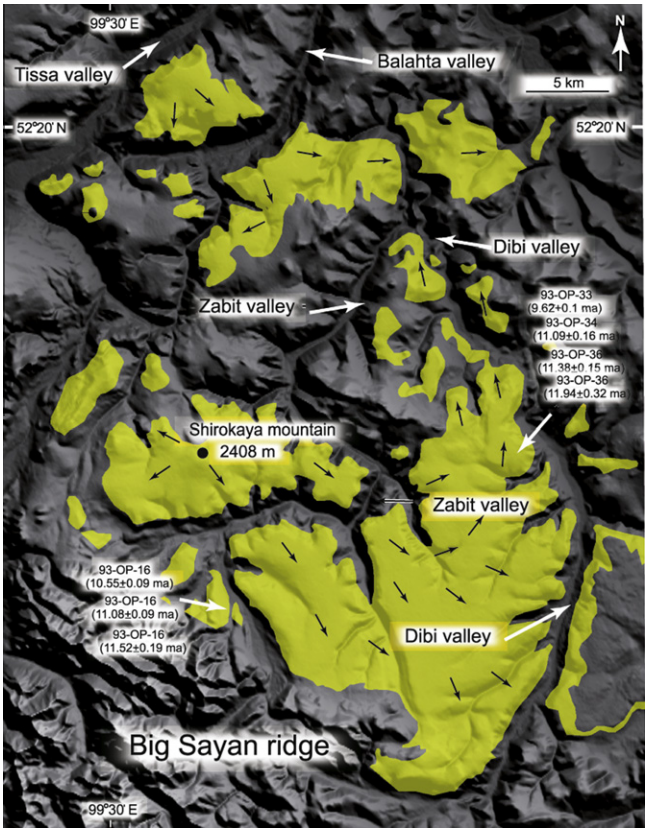

Fig. 9. SRTM® topographic map of the Neogene lavas (in yellow) on top of the Oka plateau between the Tissa valley and the Dibi valley (DT plateau area). Ages are from Rasskazov et al. (2000) and from Ivanov and Demonterova (2009). See Fig. 2 for location. (For interpretation of the references to color in this figure legend, the reader is referred to the web version of this article.)

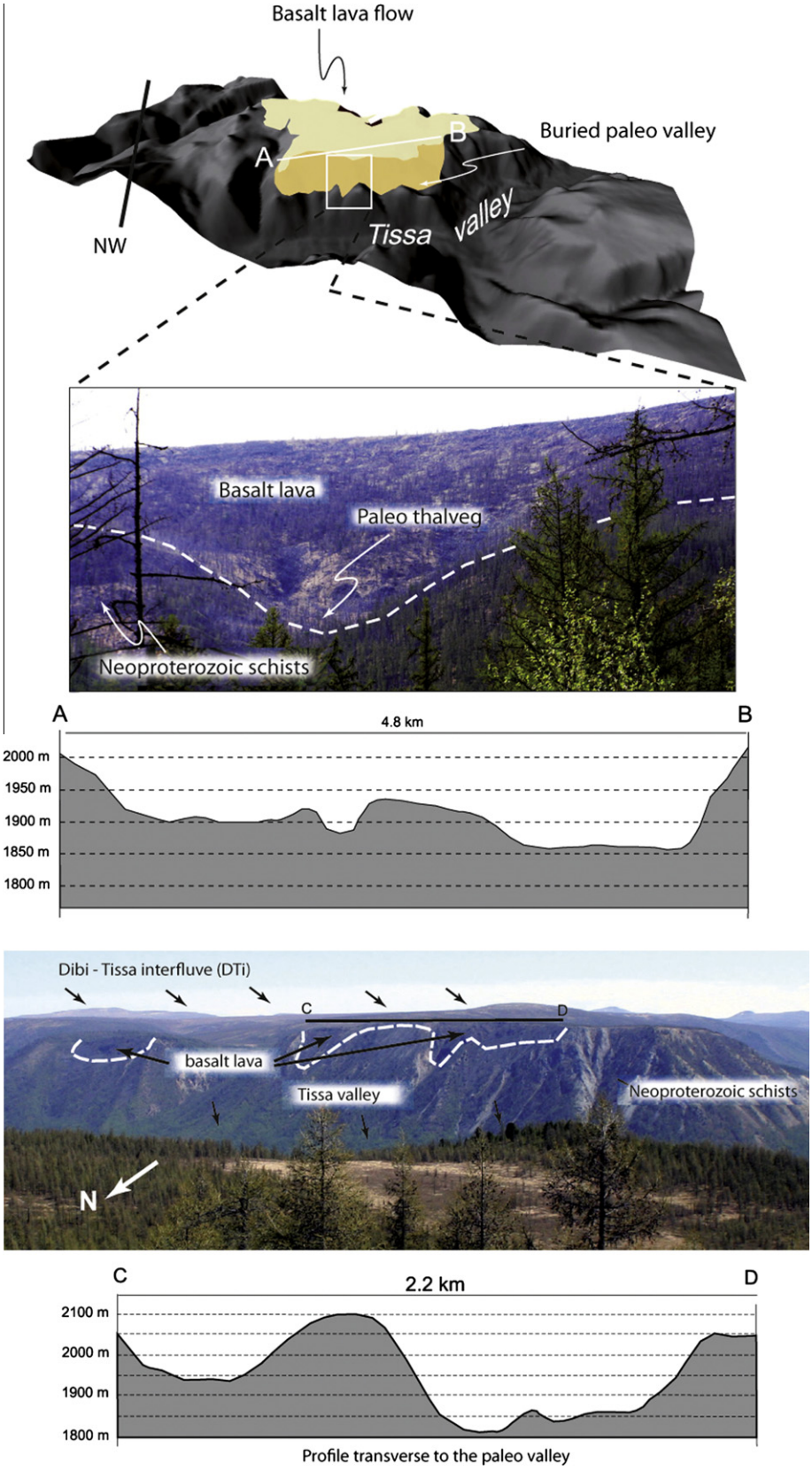

Fig. 10. Topography and pictures of the lava flow (in yellow on the topographic model) filling a 100–400 m deep and 4–5 km wide paleovalley that crosses the Tissa and Balahta present valleys. (For interpretation of the references to color in this figure legend, the reader is referred to the web version of this article.)

the actual Dibi valley. The flows are several hundred of meters thick and one of them emplaced in a 4 km wide and 350–400 m deep valley.

To summarize, in early Miocene the Oka plateau was affected by a series of relatively large (up to 5 km), 100–400 m deep valleys separating relatively flat surfaces with some 100–200 m high hills.

Please cite this article in press as: Jolivet, M., et al. Geomorphic Mesozoic and Cenozoic evolution in the Oka-Jombolok region (East Sayan ranges, Siberia). Journal of Asian Earth Sciences (2011), doi:10.1016/j.jseaes.2011.09.017

Further information on the Neogene topography of the Oka region are reported by Obruchev (1946) and Grossvald (1965) from the study of the Dozor-Urda-Hyrpis basalt series in the Tissa valley (Figs. 2 and 12). The section is composed of several lava flows interbedded with argillite and lignite lens. The whole section lies on Neoproterozoic schists. Immediately above the basement a 6 m thick bed of sand and gravel yield an important flora. These sediments are capped by a 60 m thick volcanic tuff itself covered by an about 5 m thick bed of fined grained, argillaceous sandstone with fragments of volcanic tuff and quartz pebbles. Finally the whole section is covered by a thick pile of basaltic flows dated at 7.9 ± 0.9 Ma (Rasskazov et al., 2000).

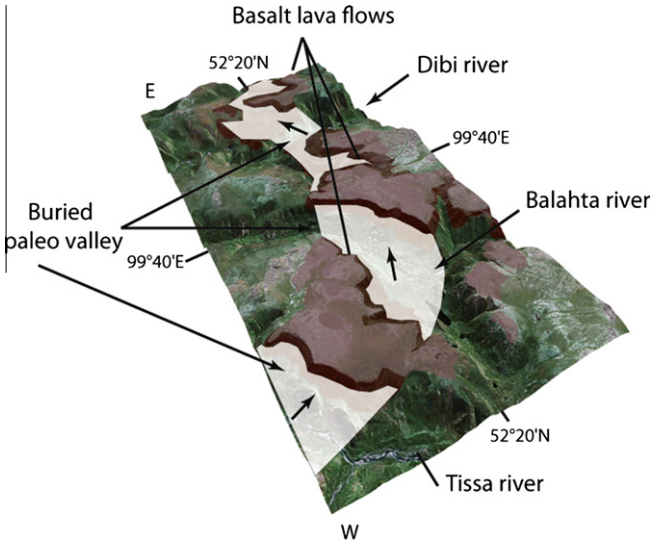

Fig. 11. Topographic reconstruction of the paleovalley across the Tissa–Balahta area.

The flora preserved inside the sedimentary beds is mostly composed of fragments of wood (*Pinus sp.*, *Pisea sp.*, and *Tauga sp.*) (Obruchev, 1946). Pollen assemblages indicate a change from vegetation dominated by deciduous trees at the base of the section to vegetation dominated by coniferous trees at the top of the section. This change is interpreted either as a general climate change or as a more local cooling due to the large amount of pyroclastic dust in the atmosphere (Obruchev, 1946). Overall, floristic studies indicate that during Miocene times the Oka region represented a large plain covered mostly by deciduous trees and some marshes. To the south a mountainous area (in place of the actual Big Sayan ridge) was covered with coniferous trees (*Abies, Pinus cembra* and *Tsuga*) that invaded the Oka plateau when the climate started to cool down either for local or regional reasons. The plain was drained by a river network forming 100–400 m deep, up to 5 km wide valleys. The relief to the south prevented the lava flows to reach further south from the actual Tissa valley. The paleo-Sentsa and paleo-Jombolok valleys probably captured the lava flows issued from the Oka plateau blocking their propagation towards the north.

Finally the last magmatic episode, from Pliocene to probably Holocene produced large lava flows such as the one filling the Khi-Gol and Jombolok valleys (up to 140 m thick). Following the work of Ivanov et al. (2011), the main lava flow in the Jombolok valley is 7130 ± 140 years old. However, several flows are piled up in the basin and direct dating of those different flows will be needed before they can be used to calculate geomorphic parameters such as the precise Holocene incision rate (e.g. Allen et al., 2011).

6. Discussion: topographic evolution of the Oka-Jombolok region from Jurassic to present

During the Middle to Late Mesozoic the topography of most of Central Asia was characterized by a planation surface which age varies from early Jurassic in the Gobi Altay, Late Jurassic in the Tien Shan and eastern Altay and finally Late Cretaceous–Paleogene in

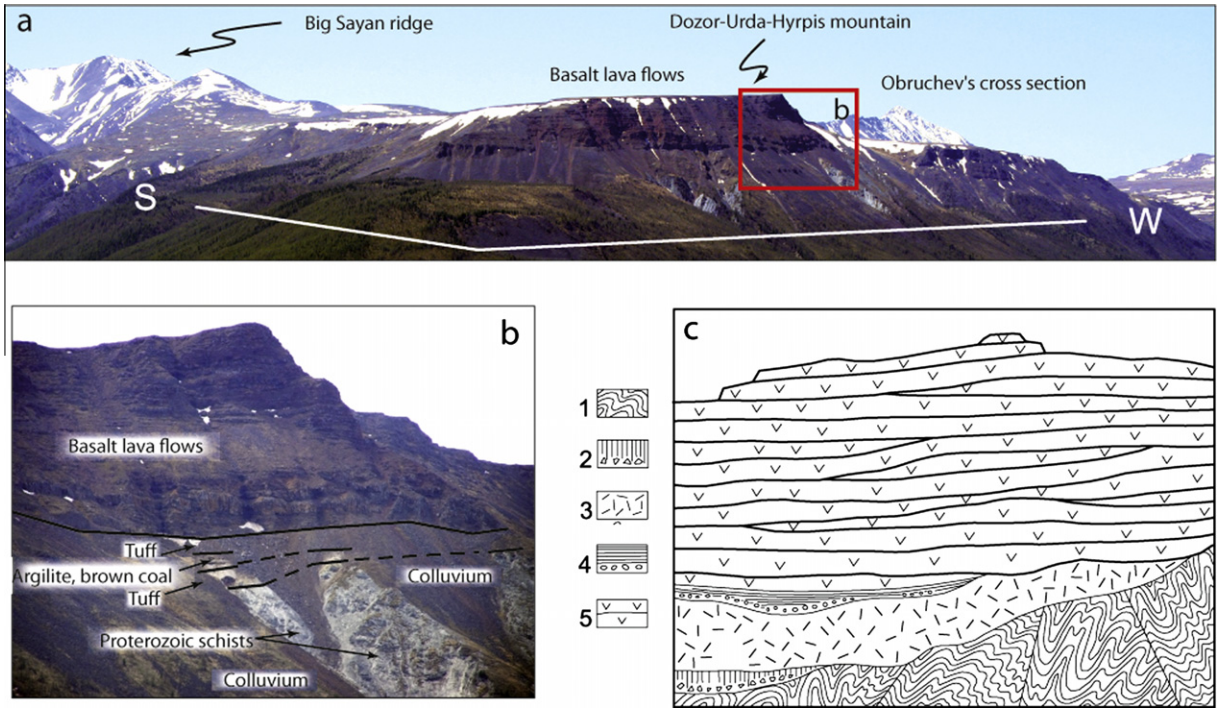

Fig. 12. General view (a) and details (b and c) of the Dozor-Urda-Hyrpis basalt series in the Tissa valley. 1: Neoproterozoic schists. 2: Colluvium. 3: Volcanic tuff. 4: Sediments (argilite and coal). 5: Basalt flows. See text for discussion and Fig. 2 for location.

Please cite this article in press as: Jolivet, M., et al. Geomorphic Mesozoic and Cenozoic evolution in the Oka-Jombolok region (East Sayan ranges, Siberia). Journal of Asian Earth Sciences (2011), doi:10.1016/j.jseaes.2011.09.017

northwest Altay (e.g. Burbank et al., 1999; Allen et al., 2001; Cunningham et al., 2003; Jolivet et al., 2007, 2010; Vassallo et al., 2007b; De Grave et al., 2008).

The topography of the East Sayan ranges clearly results from a strong reworking of the pre-Oligocene topography by the Tertiary tectonic phase. However, the apatite fission track results obtained in this work indicate that some of the topography and especially the large plateau areas represent remnants of the Late Mesozoic–Early Cenozoic (at least 140–120 Ma) surface. Similar fission track ages have been obtained by De Grave and Van den haute (2002) and De Grave et al. (2008) in northeast Altay near Lake Teletskoye and on the Chulyshman plateau. Unlike our own results most of these data show a two-stages cooling history with a first Late Jurassic–Cretaceous cooling event followed by a Late Cretaceous–Paleogene isothermal stage and a final Neogene to present cooling event.

The authors interpret the first cooling stage as resulting from the far-field effects of the closure of the Mongol-Okhotsk ocean (e.g. Kravchinsky et al., 2002; Metelkin et al., 2007, 2010) that potentially affected the whole Sayan, Baikal and Transbaikal regions (Ermikov, 1994; Delvaux et al., 1995, 1997; Dobretsov et al., 1996; Zorin, 1999; Jolivet et al., 2009). Studying the Mesozoic sediments of the Kuznetsk basin, northwest of the West Sayan ranges Davies et al. (2010) reported at least three episodes of deformation in Middle Triassic–Early Jurassic, in Late Jurassic–Early Cretaceous and in Late Cretaceous or Cenozoic. However, while the Middle Triassic–Early Jurassic sediments are formed by coarse conglomerates clearly indicating strong uplift and erosion in the hinterland, the Cretaceous series are represented by thin, fine-grained deposits suggesting no uplift in the hinterland. Le Heron et al. (2008) also reported the development of a Middle Jurassic peneplanation surface in the North Altay–West Sayan area. A phase of extensive regression during the Early Cretaceous in the Mariinsk–Krasnoyarsk region of the West Siberian basin (Fig. 1) associated to coarse clastic sediments indicates renewed uplift and erosion around the southern edges of the basin (Le Heron et al., 2008). Finally, along the eastern edge of the Siberian craton, a Late Jurassic–Early Cretaceous episode of strong cooling is also reported by Van der beek et al. (1996) in the Olkhon island and on the eastern side of Lake Baikal. Late Jurassic cooling also affected the southwestern part of the Patom range, north of Lake Baikal (Jolivet et al., 2009). In the eastern Transbaikal region, around the Early–Middle Jurassic boundary flyshoïd sediments gave way to continental molasse deposits (Mushnikov et al., 1966; Ermikov, 1994; Zorin, 1999) indicating the possible closure of the Mongol–Okhotsk ocean in that region. During Middle–Late Jurassic, intermountain basins accumulated calc-alkaline and sub-alkaline magmatism interbedded with continental sediments (Mushnikov et al., 1966). However, Enkin et al. (1992) and Metelkin et al. (2007, 2010) calculated using paleomagnetic data that by late Middle–early Late Jurassic the Mongol-Okhotsk ocean was not completely closed and that this closure only occurred in Early Cretaceous. This Early Cretaceous estimate for the closure of the Mongol-Okhotsk ocean seems nonetheless incompatible with the contemporaneous formation of rift basins and metamorphic core complexes in the Transbaikal and northern Mongolia region (e.g. Zorin, 1999; Donskaya et al., 2008; Daoudene et al., in press).

To summarize, Middle Jurassic–Early Cretaceous deformation probably linked to the closure of the Mongol-Okhotsk ocean and the collision between Mongolia and Siberia did occur in the Altai-Sayan, Baikal and north Mongolia region. However, the precise timing of this collision remains to be assessed to confidently relate the Late Jurassic–Early Cretaceous cooling observed in the East Sayan to this geodynamic phase.

The Late Cretaceous-Paleogene isothermal stage observed by De Grave and Van den haute (2002) and De Grave et al. (2008) is interpreted by these authors as corresponding to the end of the planation process and the development of a lateritic-kaolinic weathering crust similar in type and age to the one observed in some areas of the East Sayan ranges (Mats, 1993; Kashik and Masilov, 1994; Logatchev et al., 2002; Dehandschutter et al., 2002). Such a weathering crust is also reported from further east in the Transbaikal area (Mats, 1993). While rapid cooling outside the apatite fission track partial annealing zone during the Cretaceous does not allow imaging a possible Late Cretaceous–Paleogene isothermal stage in the Olkhon region (Van der Beek et al., 1996), this one is observed in the samples from southwest Patom and east Baikal (Van der beek et al., 1996; Jolivet et al., 2009). However, our fieldwork in the Oka plateau area did not reveal any occurrence of such a weathering crust and the Late Cretaceous–Paleogene isothermal stage observed in northwest Altay is not represented in the cooling history obtained for the Oka plateau (Fig. 5 and 6). We cannot rule out the possibility that a weathering crust formed at some stage on the Oka plateau and was subsequently eroded away during the Cenozoic general uplift phase. However, based on the complete absence of remnants of this crust, on the slow, continuous cooling pattern observed in the apatite fission track cooling history consistent with the erosion rates derived from the ^{10}Be data on the Oka plateau (12–20 m/Ma) we propose that this crust never develop in the Oka-Jombolok area.

By protecting the pre-Miocene surface the lava flows that cover an extensive surface of the Oka plateau provide a unique opportunity to describe this peneplain at least in the East Sayan region. While many researchers describe the occurrence of a peneplanation surface in Central Asia during the Mesozoic, no large-scale detailed geomorphologic description of this surface has been reported up to now. The occurrence of wide (up to 5 km) but relatively shallow (100–400 m) valleys separating plateaus indicate that in early Miocene this surface was not perfectly flattened by erosion and that a coherent drainage pattern existed. However sediments indicate that the Cenozoic uplift initiated during Oligocene times in the East Sayan (Strelkov and Vdovin, 1969; Arsentyev, 1975; Mazilov et al., 1993) so probably slightly before the onset of the strong magmatic episode that generated the Oka–Azas lavas. In the West Siberian basin the absence of significant post-Oligocene sediments (Kontorovich, 1975; Vyssotski et al., 2006) associated to Oligocene (around 25 Ma) folds and a still ongoing phase of subtle, long wavelength surface deformation have been attributed to the far field effects of the India Asia collision (Allen and Davies, 2007). It is thus possible that the early Miocene valleys were newly acquired features on a previously flat surface. This would be consistent with the fact that no Cretaceous or Paleogene sediments have been described in these valleys (some of them might be present but either not accurately dated or not exposed). The general slope towards the east (either NE or SE) indicated by the flow direction of the lavas in the eastern Oka plateau (Vdovin, 1976; Ivanov and Demonterova, 2010) or the progressive deepening of the paleovalley crossing the Tissa and Balahta valleys (this study) is consistent with a base level situated on the Siberian platform. Finally the downcutting of valleys during the Oligocene is also coherent with the plateaus themselves: if a permanent drainage network formed by such valleys had existed since the Mesozoic it would have been difficult to develop flat areas in-between the valleys and the topography would have rather been composed of small hills separated by valleys.

If the paleovalleys that cut through the plateau can possibly be Cenozoic features, the small 200–300 m high hills preserved on top of the plateau surfaces are more difficult to explain in terms of rejuvenated topography. As indicated previously, those hills form NW–SE trending ridges that separate the Miocene lava flows and were thus pre-existing to the lavas. They do not seem to be connected to the paleovalleys but are rather inselbergs preserved on the overall planted surface.

Please cite this article in press as: Jolivet, M., et al. Geomorphic Mesozoic and Cenozoic evolution in the Oka-Jombolok region (East Sayan ranges, Siberia). Journal of Asian Earth Sciences (2011), doi:10.1016/j.jseaes.2011.09.017

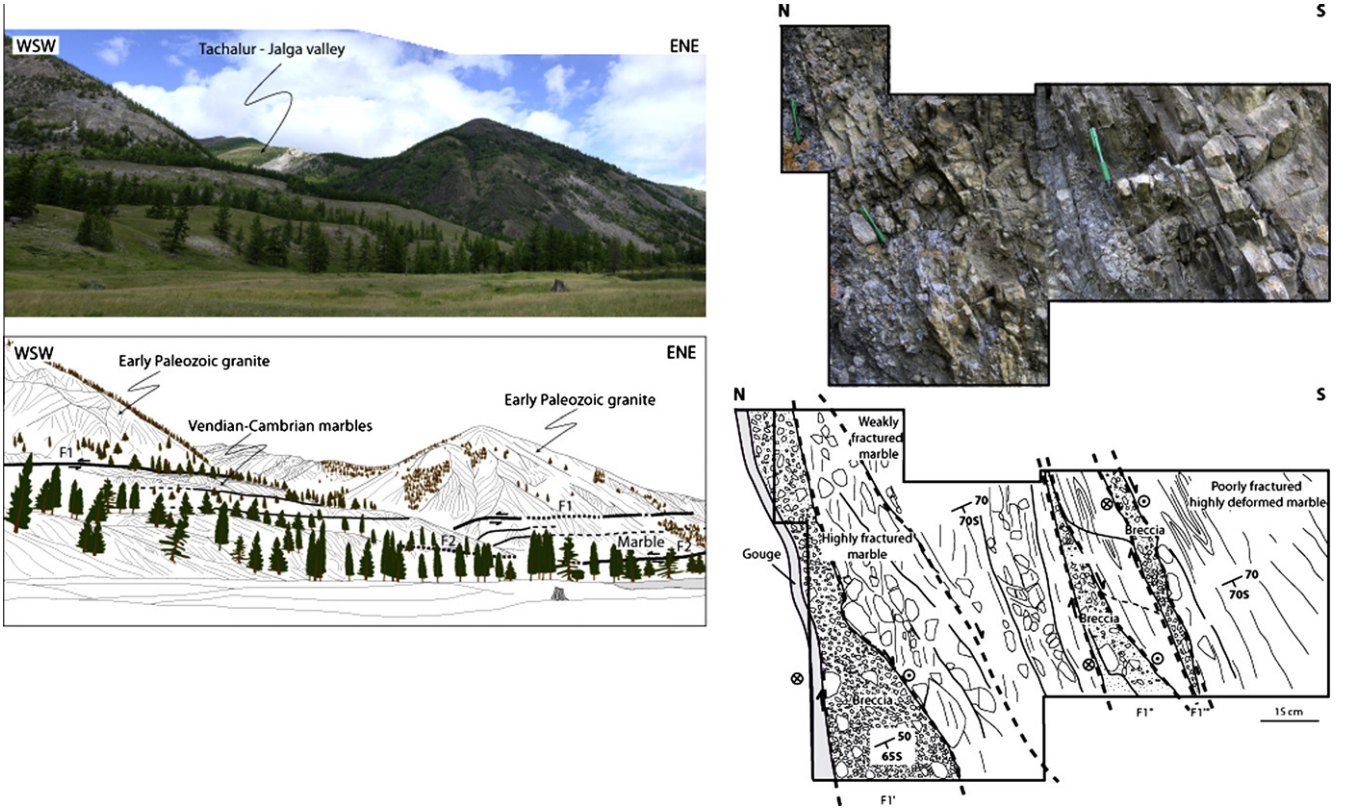

Fig. 13. (a) Picture (top) and drawn interpretation of the Oka-Jombolok fault near the outlet of the Tachalur-Jalga river incision. The fault is separated in two major planes F1 and F2 plus a number of secondary, paralell segments. (b) General overview of the fault planes within the Vendian–Cambrian marble unit at the Tachalar-Jalga river point. Foliation trends are indicated as well as the degree of fracturing of the marble. Thick dashed lines underline the three main faults. Note the occurrence of previously formed ductile structures and of gouge level on the left part of the outcrop.

The late Mesozoic topography of the Oka-Jombolok region may thus be represented by a generally flat peneplanation surface with some 200–300 m high inselbergs and a poorly developed drainage pattern. This topography developed after the Late Jurassic–Early Cretaceous general exhumation event that affected most of the North Altay, Sayan, Transbaikal and South Patom area. However, unlike in other regions, constant mechanical erosion (which process remains to be understood) prevented the formation of a lateritic-kaolinic weathering crust.

During the late Cenozoic the Mesozoic peneplanation surface was also dismantled by movements along major faults such as the Jombolok fault. This very complex tectonic lineament revealed several episodes of movement, with different directions of motion superimposed on the same fault planes. Arzhannikova et al. (2011) recently showed that vertical movements occurred along the Oka-Jombolok fault during Pliocene to Pleistocene, leading to a roughly 400 m uplift of the Kropotkin range above the level of the Oka plateau. However, this uplift seems to decrease towards the west of the Jombolok basin where remnants of the peneplanation surface are preserved (at different altitudes) on both sides of the Oka-Jombolok fault (Fig. 3). This is consistent with the mostly horizontal fault kinematic observed on the various outcrops in the Tachalur–Jalga valley (Fig. 13). The vertical motion along the fault would thus be restricted to limited segments as already suggested by Arzhannikova et al. (2011). Those observations indicate that the Cenozoic topography of the East Sayan region evolves following two modes:

– A short wavelength relief is formed locally along discrete tectonic structures such as the Oka extension zone or the Tunka range and basin. This highly dissected relief forms the most prominent structures. However, uplift and denudation are localized along the faults and in the glacial valleys, preserving the slow "background" erosion signal of the plateau remnants.
– A general uplift of the region occurs at a much longer wavelength uplifting the preserved remnants of the Mesozoic peneplanation surface to altitudes between 500–600 m west of the East Sayan ranges and 1800–2200 m in the central and southern area of the East Sayan ranges. The mechanism at the origin of that uplift is still to be understood. Part of it may be due to local underplating of mantle-derived magmas but several evidences such as the variations in time and space of the uplift suggest that it is not the only and probably not the main mechanism but that subtle deformation associated to the far field effects of the India–Asia collision may also be implied (Allen and Davies, 2007). This long-wavelength uplift probably caused the downcutting of the Cenozoic valleys (the initial pre-Miocene paleovalleys but also some of the actual ones) but its impact on the dismembering of the Mesozoic surface is limited.

7. Conclusions

The planation surface still preserved on the Oka plateau developed during the Mesozoic following the dismantling of Middle Triassic–Early Jurassic and probably Late Jurassic–Early Cretaceous relief. In that respect, the large-scale peneplanation process observed in Central Asia during the Mesozoic may be diachronous from south to north. Furthermore, unlike its equivalent in Goby Altay, Altay or West Sayan, the East Sayan planation surface has been constantly rejuvenated by slow erosion since its formation (the topography remained flat but the surface was constantly stripped away by erosion). The long-term exhumation rates (about

Please cite this article in press as: Jolivet, M., et al. Geomorphic Mesozoic and Cenozoic evolution in the Oka-Jombolok region (East Sayan ranges, Siberia). Journal of Asian Earth Sciences (2011), doi:10.1016/j.jseaes.2011.09.017

150 Myrs) of about 17.5 m/Myrs obtained from apatite fission track thermochronology on the Oka plateau are coherent with the shorter term (less than 1 Ma) erosion rates (between 12 and 20 m/Myrs) derived from ^{10}Be analysis implying that the mean erosion rate on the plateau remained largely constant through time. This erosion prevented the formation of a lateritic–kaolinic weathering crust on the surface during Late Cretaceous–Paleogene as observed on numerous other plateaus in southern Siberia. In that respect the Oka plateau is a unique feature where the "background" erosion related to the mean climatic erosional mechanism can be observed. The concordance between climatic erosion rates over hundreds of million years and over the last few hundreds of thousand years is striking.

The planation surface on which only some small 200–300 m high hills but no structured drainage network remained, started to be affected by river incision during the Oligocene–early Miocene. This renewed incision is probably linked to a large-scale long-wavelength uplift of the region and the development of a general slope towards the Siberian platform. The newly formed valley as well as the surrounding flat surfaces were then partially sealed by Miocene mantle-derived lavas which driving mechanism remains to be understood.

Finally, from Pliocene to Present the East Sayan region has been affected by transpressional and transtensional movements localized along major inherited fault zones such as the Oka-Jombolok fault. These last tectonic movements further dismembered the Mesozoic planation surface by creating a short-wavelength relief formed by ridges (such as the Kropotkin ridge) and basins (such as the Jombolok basin).

The complex morphology of the East Sayan ranges thus derives both from a strong reworking of a Mesozoic planation surface and the development of new Tertiary transpressional and transtensional structures. However, our results demonstrate that this morphology remained relatively simple until the Pliocene onset of localized deformation. Where it is preserved the planation surface can be used as a reference level to estimate the amount of post Pliocene differential uplift across the various faults. Finally, the Oligocene–early Miocene long wavelength uplift remains to be quantified and explained.

Acknowledgments

This work was financed by the Russian Fund for Basic Research Number 05-05-66812 and by the French-Russian Programme International de Coopération Scientifique – Russian Fund for Basic research Project Number 4881 – 09-05-91052. R.B. thanks F. Chauvet for his assistance in ^{10}Be chemistry preparation and M. Arnold, G. Aumaître, K. Keddadouche for their valuable assistance during ^{10}Be measurements at the ASTER AMS national facility (CEREGE, Aix-en-Provence) which is supported by the INSU/CNRS, the French Ministry of Research and Higher Education, the IRD and the CEA. T. Donskaya and M. Allen provided helpful comments to improve the initial manuscript.

References

Allen, M.B., Davies, C.E., 2007. Unstable Asia: active deformation of Siberia revealed by drainage shifts. Basin Research 19, 379–392.

Allen, M.B., Aslop, G.I., Zhemchuzhnikov, V.G., 2001. Dome and basin refolding and transpressive inversion along the Karatau fault system, southern Kazakstan. Journal of the Geological Society, London 168, 83–95.

Allen, M.B., Mark, D.F., Kheirkhah, M., Barfod, D., Emami, M.H., Saville, C., 2011. ^{40}Ar/^{39}Ar dating of Quaternary lavas in northwest Iran: constraints on the landscape evolution and incision rates of the Turkish–Iranian plateau. Geophysical Journal International 185, 1175–1188.

Arsentyev, V.P., 1975. Explanatory Note for the Geological Map 1:200 000, East Sayan series, Sheet N-47-XXVIII. VSEGEI, Moscow, 76 p. (in Russian).

Artemyev, M.E., Genshaft, Yu.S., Saltykovskii, A.Y., 1978. Correlation of neotectonics and magmatism of the Mongolian People's Republic with mantle component of the gravity field. Doklady Akademii Nauk SSSR 241, 1303–1306 (in Russia).

Arzhannikova, A., Arzhannikov, S., Jolivet, M., Vassallo, R., Chauvet, A., 2011. Pliocene to Quaternary deformation in South East Sayan (Siberia): initiation of the Tertiary compressive phase in the southern termination of the Baikal Rift System. Journal of Asian Earth Science 40, 581–594. doi:10.1016/j.jseaes.2010.10.11.

Barbarand, J., Carter, A., Wood, I., Hurford, T., 2003. Compositional and structural control of fission-track annealing in apatite. Chemical Geology 198, 107–137.

Barruol, G., Deschamps, A., Déverchère, J., Mordvinova, V.V., Ulziibat, M., Perrot, J., Artemiev, A.A., Dugarmaa, T., Bokelmann, G.H.R., 2008. Upper mantle flow beneath and around the Hangay dome, Central Mongolia. Earth Planetary Sciences Letter 274, 221–233.

Barry, T.L., Saunders, A.D., Kempton, P.D., Windley, B.F., Pringle, M.S., Dorjnamjaa, D., Saandar, S., 2003. Petrogenesis of Cenozoic basalts from Mongolia: evidence for the role of asthenospheric versus metasomatised mantle sources. Journal of Petrology 44, 55–91.

Brown, E.T., Edmond, J.M., Raisbeck, G.M., Yiou, F., Kurz, M.D., Brook, E.J., 1991. Examination of surface exposure ages of Antarctic moraines using in-situ produced ^{10}Be and ^{26}Al. Geochimica and Cosmochimica Acta 55, 2269–2283.

Brown, E.T., Stallard, R.F., Larsen, M.C., Raisbeck, G.M., Yiou, F., 1995. Denudation rates determined from the accumulation of in situ produced ^{10}Be in the Luquillo experimental forest, Puerto-Rico. Earth Planetary Sciences Letter 129, 193–202.

Burbank, D.W., McLean, J.K., Bullen, M., Abdrakhmatov, K.Y., Miller, M.M., 1999. Partitioning of intermontane basins by thrust-related folding, Tien Shan, Kyrgyzstan. Basin Research 11, 75–92.

Burtner, R.L., Nigrini, A., Donelick, R.A., 1994. Thermochronology of lower Cretaceous source rocks in the Idaho–Wyoming Thrust Belt. American Association of Petroleum Geologists Bulletin 78, 1613–1636.

Chipizubov, A.V., Serebrennikov, S.P., 1990. Strike-slip paleoseismodislocations in the East Sayan. Doklady Akademii Nauk SSSR 311, 446–450 (in Russian).

Chmeleff, J., von Blanckenburg, F., Kossert, K., Jacob, D., 2010. Determination of the ^{10}Be half-life by multicollector ICP-MS and liquid scintillation counting. Nuclear Instruments & Methods in Physics Research Section B 268, 192–199.

Corrigan, J., 1991. Inversion of apatite fission track data for thermal history information. Journal of Geophysical Research 96, 10347–10360.

Cunningham, W.D., 2001. Cenozoic normal faulting and regional doming in the southern Hangay region, central Mongolia: implications for the origin of the Baikal rift province. Tectonophysics 331, 389–411.

Cunningham, D., Dijkstra, A.H., Howard, J., Quarles, A., Badarch, G., 2003. Active intraplate strike-slip faulting and transpression uplift in the Mongolian Altai. Geological Society Special Publications 210, 65–87.

Daoudene, Y., Ruffet, G., Cocherie, A., Ledru, P., Gapais, D., in press. Timing of exhumation of the Ereendavaa metamorphic core complex (north-eastern Mongolia) – U–Pb and ^{40}Ar/^{39}Ar constraints. Journal of Asian Earth Sciences, doi:10.1016/j.jseaes.2011.04.009.

Davies, C., Allen, M.B., Buslov, M.M., Safonova, I., 2010. Deposition in the Kuznetsk basin, Siberia: insights into the Permian–Triassic transition and the Mesozoic evolution of Central Asia. Palaeogeography, Palaeoclimatology, Palaeoecology 295, 307–322.

De Grave, J., Van den Haute, P., 2002. Denudation and cooling of the Lake Teletskoye Region in the Altai Mountains (South Siberia) as revealed by apatite fission-track thermochronology. Tectonophysics 349, 145–159.

De Grave, J., Dehandschutter, B., Van den Haute, P., Buslov, M.M., Boven, A., 2003. Low-temperature thermo-tectonic evolution of the Altai-Sayan Mountains, South Siberia, Russia. Geophysical Research Abstracts 5, 11996.

De Grave, J., Van den haute, P., Buslov, M.M., Dehandschutter, B., Glorie, S., 2008. Apatite fission-track thermochronology applied to the Chulyshman Plateau, Siberian Altai Region. Radiation Measurements 43, 38–42.

Dehandschutter, B., Vysotsky, E., Delvaux, D., Klerkx, J., Buslov, M.M., Seleznev, V.S., De Batist, M., 2002. Structural evolution of the Teletsk graben (Russian Altai). Tectonophysics 351, 139–167.

Delvaux, D., Moeys, R., Stapel, G., Melnikov, A., Ermikov, V., 1995. Palaeostress reconstructions and geodynamics of the Baikal region, Central Asia, Part I. Palaeozoic and Mesozoic pre-rift evolution. Tectonophysics 252, 61–101.

Delvaux, D., Moeys, R., Stapel, G., Petit, C., Levi, K., Miroshnichenko, A., Ruzzhich, V., San'kov, V., 1997. Paleostress reconstructions and geodynamics of the Baikal region, Central Asia, Part 2. Cenozoic rifting. Tectonophysics 282, 1–38.

Dobretsov, N.L., Buslov, M.M., Delvaux, D., Berzin, N.A., Ermikov, V.D., 1996. Meso- and Cenozoic tectonics of the Central Asian mountain belt: effects of lithospheric plate interaction and mantle plumes. International Geology Review 38, 430–466.

Donelick, R.A., 1991. Crystallographic orientation dependence of mean etchable fission track length in apatite: an empirical model and experimental observation. American Mineralogist 76, 83–91.

Donelick, R.A., 1993. A Method of Fission Track Analysis Utilizing Bulk Chemical Etching of Apatite. US Patent Number 6267,274.

Donelick, R.A., Ketcham, R.A., Carlson, W.D., 1999. Variability of apatite fission-track annealing kinetics: II. Crystallographic orientation effects. American Mineralogist 84, 1224–1234.

Donskaya, T.V., Windley, B.F., Mazukabzov, A.M., Kröner, A., Sklyarov, E.V., Gladkochub, D.P., Ponomarchuk, V.A., Badarch, G., Reichow, M.K., Hegner, E., 2008. Age and evolution of late Mesozoic metamorphic core complexes in southern Siberia and northern Mongolia. Journal of the Geological Society of London 165, 405–421. doi:10.1144/0016-76492006-162.

Please cite this article in press as: Jolivet, M., et al. Geomorphic Mesozoic and Cenozoic evolution in the Oka-Jombolok region (East Sayan ranges, Siberia). Journal of Asian Earth Sciences (2011), doi:10.1016/j.jseaes.2011.09.017

Dunkl, I., 2002. TRACKKEY: a Windows program for calculation and graphical presentation of fission track data. Computers and Geosciences 28, 3–12.
Dunne, J., Elmore, D., Muzikar, P., 1999. Scaling factors for the rates of production of cosmogenic nuclides for geometric shielding and attenuation at depth on sloped surfaces. Geomorphology 27, 3–11.
Enkin, R., Yang, Z., Chen, Y., Courtillot, V., 1992. Paleomagnetic constraints on the geodynamic history of the major blocks of China from the Permian to the Present. Journal of Geophysical Research 97, 13953–13989.
Ermikov, V.D., 1994. Mesozoic precursors of rift structures of Central Asia. Bulletin du Centre de Recherches Exploration–Production Elf Aquitaine 18, 123–134.
Galbraith, R.F., 2005. Statistics for Fission Track Analysis. Chapman & Hall/CRC, Boca Raton.
Galbraith, R.F., Laslett, G.M., 1993. Statistical models for mixed fission track ages. Nuclear Tracks and Radiation Measurements 21, 459–470.
Gallagher, K., Charvin, K., Nielsen, S., Sambridge, M., Stephenson, J., 2009. Markov chain Monte Carlo (MCMC) sampling methods to determine optimal models, model resolution and model choice for Earth Science problems. Marine and Petroleum Geology 26, 525–535.
Green, P.F., 1981. "Track-in-track" length measurements in annealed apatites. Nuclear Tracks 5, 77–86.
Green, P.F., 1985. A comparison of zeta calibration baselines in zircon, sphene and apatite. Chemical Geology 58, 1–22.
Green, P.F., Durrani, S.A., 1978. A quantitative assessment of geometry factors for use in fission track studies. Nuclear Tracks 2, 207–213.
Green, P.F., Duddy, I.R., Laslett, G.M., Hegarty, K.A., Gleadow, A.J.W., Lovering, J.F., 1989. Thermal annealing of fission tracks in apatite 4. Quantitative modelling techniques and extension to geological timescales. Chemical Geology 79, 155–182.
Grossvald, M.G., 1965. Topographic development of the Sayan-Tuva Upland. Nauka, Moscow, 166 p. (in Russian).
Gusev, G.S., Khain, V.Y., 1996. On relations between the Baikal-Vitim, Aldan Stanovoy, and Mongol-Okhotsk terranes (south of mid-Siberia). Geotectonics 29, 422–436.
Le Heron, D.P., Buslov, M.M., Davies, C., Richards, K., Safonova, I., 2008. Evolution of Mesozoic fluvial systems along the SE flank of the West Siberian Basin, Russia. Sedimentary Geology 208, 45–60.
Hurford, A.J., 1990. Standardization of fission track dating calibration: recommendation by the Fission Track Working Group of the I UGS. Subcomission on geochronology. Chemical Geology (Isotope Geoscience Section) 80, 171–178.
Hurford, A.J., Green, P.F., 1983. The zeta age calibration of fission-track dating. Chemical Geology 1, 285–317.
Ionov, D.A., O'Reilly, S.Y., Ashchepkov, I.V., 1995. Feldspar-bearing lherzolite xenoliths in alkali basalts from Hamar-Daban, southern Baikal region, Russia. Contributions to Mineralogy and Petrology 122, 174–190.
Ivanov, A.V., Demonterova, E.I., 2009. Tectonics of the Baikal Rift Deduced from Volcanism and Sedimentation: A Review Oriented to the Baikal and Hovsgol Lake Systems. In: Müller, W.E.G., Grachev, M.A. (Eds.), Biosilica in Evolution, Morphogenesis, and Nanobiotechnology. Progress in Molecular and Subcellular Biology, Marine Molecular Biotechnology 47, doi:10.1007/978-3-540-88552-8, Springer-Verlag, Berlin Heildelberg, 2009.
Ivanov, A.V., Demonterova, E.I., 2010. Extension in the Baikal Rift and the depth of basalt magma generation. Doklady Earth Sciences 435, 1564–1568.
Ivanov, A.V., Arzhannikov, S.G., Demonterova, E.I., Arzhannikova, A.V., Orlova, L.A., 2011. Jom-Bolok Holocene volcanic field in the East Sayan Mts., Siberia, Russia: Structure, style of eruptions, magma compositions and the first radiocarbon dating results. Bulletin of Volcanology, doi:10.1007/s00445-011-04585-9.
Jolivet, M., Brunel, M., Seward, D., Xu, Zh., Yang, J., Roger, F., Tapponnier, P., Malavieille, J., Arnaud, N., Wu, C., 2001. Mesozoic and Cenozoic tectonics of the northern edge of the Tibetan plateau: fission-track constraints. Tectonophysics 343, 111–134.
Jolivet, M., Ritz, J-F., Vassallo, R., Larroque, C., Braucher, R., Todbileg, M., Chauvet, A., Sue, C., Arnaud, N., De Vicente, R., Arzhanikova, A., Arzhanikov, S., 2007. The Mongolian summits: an uplifted, flat, old but still preserved erosion surface. Geology 35, 871–874. doi:10.1130/G23758A.1.
Jolivet, M., De Boisgrollier, T., Petit, C., Fournier, M., Sankov, V.A., Ringenbach, J.-C., Byzov, L., Miroshnichenko, A.I., Kovalenko, S.N., Anisimova, S.V., 2009. How old is the Baikal Rift Zone? Insight from apatite fission track thermochronology. Tectonics 28, TC3008. doi:10.1029/2008TC002404.
Jolivet, M., Dominguez, S., Charreau, J., Chen, Y., Li, Yongan, Wang, Qingchen, 2010. Mesozoic and Cenozoic tectonic history of the Central Chinese Tian Shan: reactivated tectonic structures and active deformation. Tectonics, 29, TC6019, doi:10.1029/2010TC002712.
Kashik, S.A., Masilov, V.N., 1994. Main stages and paleogeography of Cenozoic sedimentation in the Baikal rift system (eastern Siberia). Bulletin du Centre de Recherches Exploration–Production Elf Aquitaine 18, 453–461.
Ketcham, R.A., Carter, A., Donelick, R.A., Barbarand, J., Hurford, A.J., 2007. Improved modelling of fission-track annealing in apatite. American Mineralogist 92, 789–798.
Kiselev, A.I., Popov, A.M., 1992. Asthenospheric diapir beneath the Baikal rift: petrological constraints. Tectonophysics 208, 287–295.
Kiselev, A.I., Medvedev, M.E., Golovko, G.A., 1979. Volcanism of the Baikal rift zone and problems of deep-seated magmatism. Nauka Siberian Branch, Novosibirsk, 196 p. (in Russian).
Kontorovich, A.E., 1975. Geology of Oil and Gas of West Siberia. Nedra, Moscow.
Korschinek, G., Bergmaier, A., Faestermann, T., Gerstmann, U.C., Knie, K., Rugel, G., Wallner, A., Dillmann, I., Dollinger, G., Lierse von Gosstomski, C., Kossert, K., Maiti, M., Poutivtsev, M., Remmert, A., 2010. A new value for the ^{10}Be half-life by heavy-ion elastic recoil detection and liquid scintillation counting. Nuclear Instruments & Methods 268, 187–191.
Kravchinsky, V.A., Cogné, J-P., Harbert, W.P., Kuzmin, M.I., 2002. Evolution of the Mongol-Okhotsk Ocean as constrained by new palaeomagnetic data from the Mongol-Okhotsk suture zone, Siberia. Geophysical Journal International 148, 34–57.
Kuzmichev, A.B., 2004. Tectonic history of the Tuva-Mongolian Massif: Early Baikalian, Late Baikalian and Early Caledonian stages. In: Sklyarov, E. (Ed.). Moscow, PROBEL-2000. 192 p.
Lal, D., 1991. Cosmic ray labeling of erosion surfaces: in situ nuclide production rates and erosion models. Earth Planetary Sciences Letter 104, 424–439.
Larroque, C., Ritz, J.-F., Stephan, J.-F., Sankov, V., Arjannikova, A., Calais, E., Deverchere, J., Loncke, L., 2001. Interaction compression–extension à la limite Mongolie-Sibérie: analyse préliminaire des deformations récentes et actuelles dans le basin de Tunka. Comptes Rendus de L Academie des Sciences, Paris 332, 177–184.
Logatchev, N.A., Zorin, Y.A., 1987. Evidence and causes for the two-stage development of the Baikal rift. Tectonophysics 143, 225–234.
Logatchev, N.A., Brandt, I.S., Rasskazov, S.V., et al., 2002. K–Ar Dating of the Paleocene Weathering Crust in the Baikal Region. Dokl. Akad. Nauk. 385, 797–799 (Dokl. Earth Sci. (Engl. Transl.), 2002, 385A, 648–650).
Mats, V.D., 1993. The structure and development of the Baikal rift depression. Earth Science Reviews 34, 81–118.
Mazilov, V.N., Kashik, S.A., Lomonosova, T.K., 1993. Oligocene deposits of the Tunka basin (Baikal rift zone). Russian Geology and Geophysics 8, 81–88.
McDowell, F.W., McIntosh, W.C., Farley, K.A., 2005. A precise ^{40}Ar–^{39}Ar reference age for the Durango apatite (U–Th)/He and fission-track dating standard. Chemical Geology 214, 249–263.
Merchel, S., Herpers, U., 1999. An update on radiochemical separation techniques for the determination of long-lived radionuclides via accelerator mass spectrometry. Radiochimica Acta 84, 215–219.
Merchel, S., Arnold, M., Aumaître, G., Benedetti, L., Bourles, D.L., Braucher, R., Alfimov, V., Freeman, S.P.H.T., Steier, P., Wallner, A., 2008. Towards more precise ^{10}Be and^{36}Cl data from measurements at the 10–14 level: influence of sample preparation. Nuclear Instruments & Methods in Physics Research Section B 266, 4921–4926.
Metelkin, D.V., Gordienko, I.V., Klimuk, V.S., 2007. Paleomagnetism of Upper Jurassic basalts from Transbaikalia: new data on the time of closure of the Mongol-Okhotsk Ocean and Mesozoic intraplate tectonics of Central Asia. Russian Geology and Geophysics 48, 825–834.
Metelkin, D.V., Vernikovsky, V.A., Kazansky, A.Y., Wingate, M.T.D., 2010. Late Mesozoic tectonics of Central Asia based on paleomagnetic evidence. Gondwana Research 18, 400–419.
Mushnikov, A.F., Anashkina, K.K., Oleksiv, B.I., 1966. Stratigraphy of Jurassic sediments in the eastern Trans-Baikal region (in Russian). In: Morozov, F.A. (Ed.), Bulletin of Geology and Mineral Resources of the Chita Region 2, Nedra, Moscow, pp. 57–99.
Nishiizumi, K., Imamura, M., Caffe, M.W., Southon, J.R., Finkel, R.C., McAninch, J., 2007. Absolute calibration of ^{10}Be AMS standards. Nuclear Instruments & Methods B58, 403–413.
Obruchev, S.V., 1946. Orography and geomorphology of the eastern half of East Sayan. Proceedings of the All-Union Geographical Society 78, 479–498 (in Russian).
Parfeevets, A.V., Sankov, V.A. 2006. Stress–Strain State of the Earth's Crust and Geodynamics of the Southwestern Baikal Rift System. Geo, Novosibirsk, 149 p. (in Russian).
Petit, C., Déverchère, J., 2006. Structure and evolution of the Baikal rift: a synthesis. Geochemistry, Geophysics, Geosystems 7. doi:10.1029/2006GC001265.
Petit, C., Burov, E., Tiberi, C., 2008. Strength of the lithosphere and strain localisation in the Baikal rift. Earth Planetary Sciences Letter 269, 522–528.
Polyansky, O.P., 2002. Dynamic causes for the opening of the Baikal Rift Zone: a numerical modelling approach. Tectonophysics 351, 91–117.
Rassakazov, S.V., 1993. Magmatism of the Baikal Rift System. Nauka, Novosibirsk, 288 p. (in Russian).
Rasskazov, S.V., Logatychev, N.A., Brandt, I.S., Brandt, S.B., Ivanov, A.V., 2000. Late Cenozoic geochronology and geodynamics (South Siberia - South and East Asia). Novosibirsk, Nauka, 288 p. (in Russian).
Rasskazov, S.V., Saranina, E.V., Demonterova, E.I., Maslovskaya, M.N., Ivanov, A.V., 2002. Mantle components in Late Cenozoic volcanics of the East Sayan (from Pb Sr, and Nd isotopes). Russian Geology and Geophysics 43, 1065–1079 (in Russian).
Ritz, J.-F., Vassallo, R., Braucher, R., Brown, E.T., Carretier, S., Bourlès, D., 2006. Using in situ-produced ^{10}Be to quantify active tectonics in the Gurvan Bogd mountain range(Gobi-Altay, Mongolia). In: Siame, L.L., Bourlès, D.L., Brown, E.T. (Eds.), Application of Cosmogenic Nuclides to the Study of Earth Surface Processes: the Practice and the Potential. Geol. Soc. Am. Spec. Pap. 415, 87–110, doi:10.1130/2006.2415(06).
San'kov, V.A., Chipizubov, A.V., Lukhnev, A.V., Smekalin, O.P., Miroshnichenko, A.I., Calais, E., Déverchère, J., 2004. Assessment of a large earthquake risk in the zone of Main Sayan fault using GPS geodesy and paleoseismology. Russian Geology and Geophysics 45, 1369–1376.

Please cite this article in press as: Jolivet, M., et al. Geomorphic Mesozoic and Cenozoic evolution in the Oka-Jombolok region (East Sayan ranges, Siberia). Journal of Asian Earth Sciences (2011), doi:10.1016/j.jseaes.2011.09.017

Seward, D., Spikings, R., Viola, G., Kounov, A., Ruiz, G.M.H., Naeser, N., 2000. Etch times and operator variation for spontaneous track lengths measurements in apatites: an intra-laboratory check. OnTrack 10, 16–21.

Siame, L., Bellier, O., Braucher, R., Sébrier, M., Cushing, M., Bourlès, D., Hamelin, B., Baroux, E., de Voogd, B., Raisbeck, G., Yiou, F., 2004. Local erosion rates versus active tectonics: cosmic ray exposure modelling in Provence (south-east France). Earth and Planetary Science Letters 107, 1–21.

Sobel, E.R., Seward, D., 2010. Influence of etching conditions on apatite fission-track etch pit diameter. Chemical Geology 271, 59–69.

Stone, J.O., 2000. Air pressure and cosmogenic isotope production. Journal of Geophysical Research 105, 23753–23759.

Strelkov, S.A., Vdovin, V.V., 1969. Topographic history of Siberia and the Far East. Altai-Sayan mountain area. Nauka, Moscow, 415 p. (in Russian).

Sugorakova, A.M., Yarmolyuk, V.V., Lebedev, V.I., 2003. Kainozoiskii vulkanizm Tuvy (Cenozoic volcanism of Tuva). Tuva Institute of Integrated Resource Development SB RAS (Ed.), Kyzyl, 92 p. (in Russian).

Tagami, T., 1987. Determination of zeta calibration constant for fission track dating. Nuclear Tracks and Radiation Measurements 13, 127–130.

Tiberi, C., Deschamps, A., Déverchère, J., Petit, C., Perrot, J., Appriou, D., Mordvinova, V., Dugaarma, T., Ulzibaat, M., Artemiev, A.A., 2008. Asthenospheric imprints on the lithosphere in Central Mongolia and Southern Siberia from a joint inversion of gravity and seismology (MOBAL experiment). Geophysical Journal International 175, 1283–1297.

Van der Beek, P., Delvaux, D., Andriessen, P.A.M., Levi, K.G., 1996. Early Cretaceous denudation related to convergent tectonics in the Baikal region, SE Siberia. Journal of the Geological Society of London 153, 515–523.

Vassallo, R., Ritz, J-F., Braucher, R., Jolivet, M., Carretier, S., Larroque, C., Chauvet, A., Sue, C., Todbileg, M., Bourlès, D., Arzhannikova, A., Arzhannikov, S., 2007a. Transpressional tectonics and stream terraces of the Gobi-Altay, Mongolia. Tectonics 26. doi:10.1029/2006TC002081.

Vassallo, R., Jolivet, M., Ritz, J-F., Braucher, R., Larroque, Ch., Sue, C., Todbileg, M., Javkhlanbold, D., 2007b. Uplift age and rates of the Gurvan Bogd system (Gobi-Altay) by apatite fission track analysis. Earth Planetary Sciences Letter 259, 333–346. doi:10.1016/j.epsl.2007.04.047.

Vassallo, R., Ritz, J.-F., Carretier, S., 2011. Control of geomorphic processes on 10Be concentrations in individual clasts: complexity of the exposure history in Gobi-Altay range (Mongolia). Geomorphology 135, 35–47.

Vdovin, V.V., 1976. Basic Stages for Topographic Development. Nauka, Moscow, 270 p. (in Russian).

Vermeesch, P., 2007. CosmoCalc: an Excel add-in for cosmogenic nuclide calculations. Geochemistry, Geophysics, and Geosystems 8. doi:10.1029/2006GC001530, Q08003.

VSEGEI, 1975. Geological Map 1:200 000, East Sayan Series, Sheet N-47-XXVIII, Moscow.

Vyssotski, A.V., Vyssotski, V.N., Nezhdanov, A.A., 2006. Evolution of the West Siberian Basin. Marine and Petroleum Geology 23, 93–126.

Yarmolyuk, V.V., Lebedev, V.I., Sugorakova, A.M., Bragin, V.Y., Litasov, Y.D., Prudnikov, S.T., Arakelyants, M.M., Lebedev, V.A., Ivanov, V.G., Kozlovskii, A.M., 2001. East Tuva neovolcanic zone in Central Asia: stages, products and character of volcanic activity. Volcanology and Seismology 3, 3–32 (in Russian).

Zorin, Y.A., 1981. The Baikal rift: an example of intrusion of asthenospheric material into the lithosphere as the cause of disruption of lithospheric plates. Tectonophysics 73, 91–104.

Zorin, Y.A., 1999. Geodynamics of the western part of the Mongolia-Okhotsk collisional belt, Trans-Baikal region (Russia) and Mongolia. Tectonophysics 306, 33–56.

Please cite this article in press as: Jolivet, M., et al. Geomorphic Mesozoic and Cenozoic evolution in the Oka-Jombolok region (East Sayan ranges, Siberia). Journal of Asian Earth Sciences (2011), doi:10.1016/j.jseaes.2011.09.017